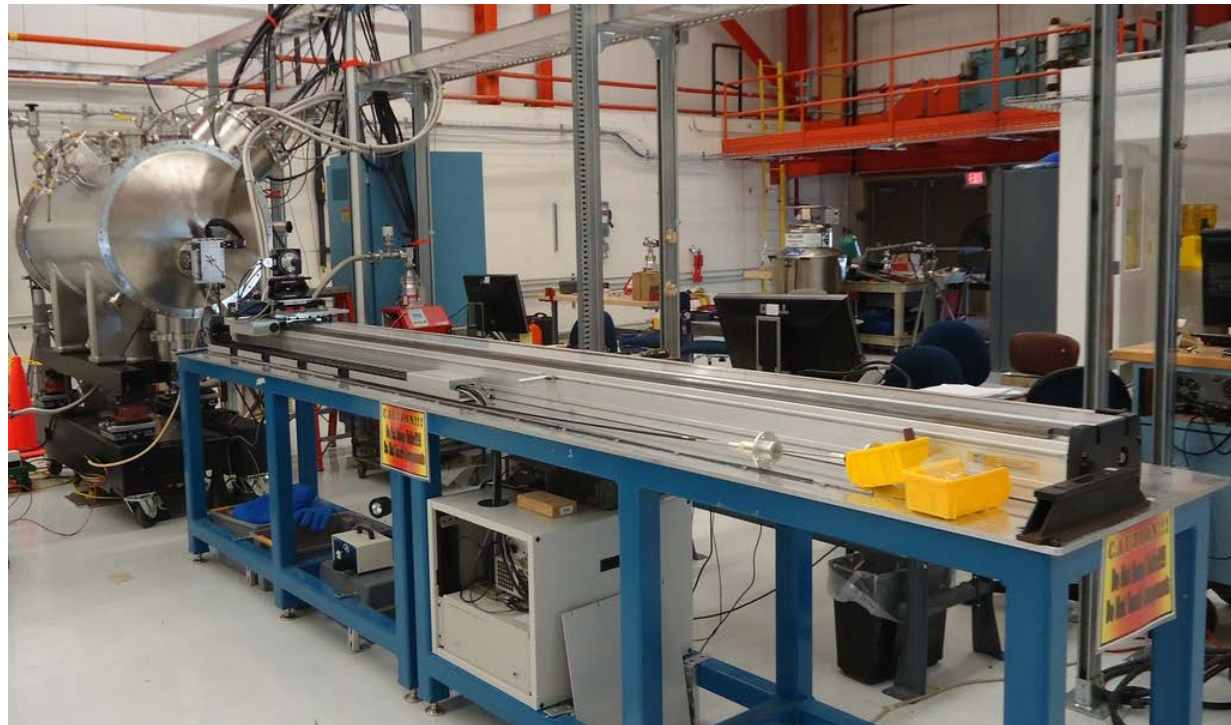


SCUO Magnetic measurement results using the horizontal measurement system

Chuck Doose, Matt Kasa
ASD Seminar August 27, 2012



Scope

- Acknowledgement of the SCU0 project contributors
- Brief description of the SCU horizontal measurement system
- Review of the SCU0 design and correction coil operation
- Typical Hall probe measurement results at 500 A
- Typical trajectory, phase errors and photon intensity spectra
- Effects of using differential end-corrector coil currents
- Hall probe measurement results as a function current and transverse position
- Rotating coil measurement results as a function of current and transverse position
- Multipoles as a function of current
- Dynamic Integrated fields during quench measured with fixed coils
- Dynamic Integrated field measurements during corrector power supply fault
- Some operational observations
- Conclusion
- References



Thanks to Some of the Contributors to the SCU0 Project

APS:

- Melike Abliz
- Neil Bartkowiak
- *Suzy Bettenhausen*
- Ralph Bechtold
- *Kurt Boerste*
- Michael Borland
- Tom Buffington
- Dana Capatina
- Jeff Collins
- Roger Dejus
- Boris Deriy
- *Chuck Doose*
- *Joel Fuerst*
- Joe Gagliano jr./sr
- Efim Gluskin
- *Quentin Hasse*
- Kathy Harkay
- ***Yury Ivanyushenkov***
- Mark Jaski
- *Matt Kasa*
- Suk Kim
- Bob Kustom
- Jie Liu
- Mike Merritt
- Liz Moog
- John Terhaar
- *Emil Trakhtenberg*
- Vadim Sajaev
- *Denise Skiadopoulos*
- Isaac Vasserman
- Joseph Xu

- *Yuko Shiroyanagi*

- Sasha Zholents

- APS Alignment Group

Visitors from Budker Institute, Russia:

- Nikolay Mezentsev
- Vasily Syrovatin
- V. Lev
- V. Tsukahov

Collaborators:

- Sasha Makarov,
Technical Division, FNAL
- John Pfothenauer, UW
Madison



SCU horizontal measurement system capabilities

- Warm bore system based on Budker Institute's wiggler measurement system. [1,2]
- Scanning Hall Probe
 - On-the-fly Hall probe measurements (2 cm/s, Δz 0.2 mm, typical z range ± 35 cm) to determine local field errors and phase errors.
 - Three sensor Hall probe (attached to carbon fiber tubing and driven by linear stage) to measure B_y and B_x simultaneously and determine the mid-plane field regardless of sensor vertical offset from magnetic mid-plane. [3]
 - Hall probes can be rotated to any fixed angle with 0.01 degree absolute accuracy. The probes can also be rotated through 360 degrees at a fixed z location.
- Stretched Wire Coil
 - Stretched wire rectangular, delta and figure 8 coils to determine static and dynamic 1st and 2nd field integrals. Wire diameter is 100 μm , coil width is 4 mm, and coil length is 3.5 m. [4]
 - Rotary stages on down-stream end of cryostat as well as on the z-axis linear stage to provide synchronized rotary motion for stretch coils.
 - Integral coil measurements performed by continuously rotating and using a software-based lock-in amplifier to determine the integrated B_y and B_x field components. [5]
 - Coils can be translated along x-axis approximately ± 1 cm to measure integrated multipole components.
- Miscellaneous
 - Ability to measure dynamic 1st and 2nd field integrals, magnet coil voltages and current during a quench.
 - Control main and corrector power supplies with accurate current read-back.
 - Ability to measure the LHe level, and temperature sensors
 - Perform excitation measurements with fixed Hall probe position

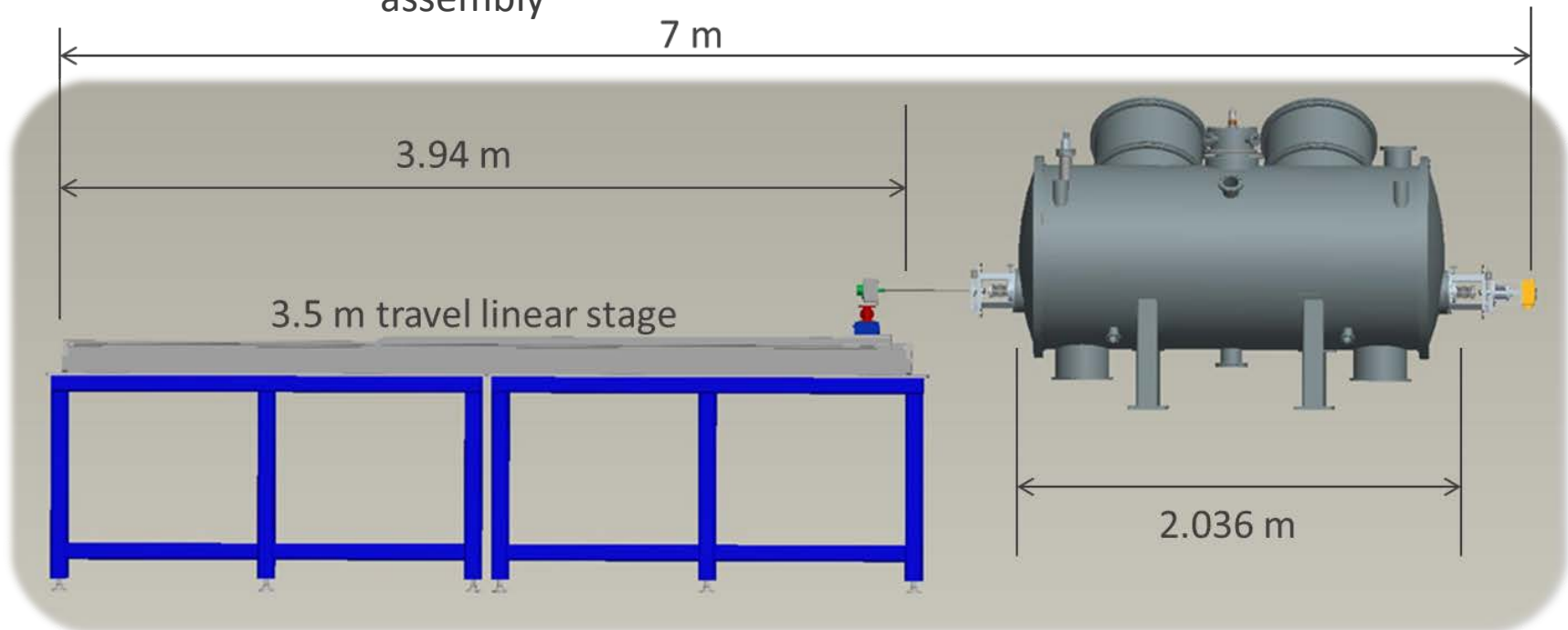
SCU Horizontal Magnetic Measurement System Specifications

- Three Arepoc Hall sensors mounted in 4 mm OD carbon fiber tubing
- Hall sensors guided by Ti tubing inside the Al beam chamber
- Integral coil consists of 1-turn 100 μm CuBe wire 4 mm width and 3.5 m length
- Coil can be configured as rectangular, delta or figure 8
- Labview based data acquisition and analysis software written by Matt Kasa
- Hall probe field resolution 0.01 Gauss
- Hall probe field accuracy ~ 0.4 Gauss
- Rotary stage resolution 0.2 mRad
- Integral Coil resolution ~ 0.1 G-cm
- Integral Coil accuracy $\sim \pm 5\%$ of measured value
- Longitudinal stage linear travel 3.5 m
- Transverse stages linear travel 1.0 cm
- Linear encoder resolution 1 μm
- Linear encoder accuracy ± 10 $\mu\text{m}/\text{m}$
- Straightness and flatness of stage 100 μm over 3.5 m travel
- Max Roll angle error ± 1 mRad
- HP Power Supply 5 Volt 890 A



SCU Horizontal Magnetic Measurement System dimensional overview

- One 3.5 m travel linear stage
- Three ± 1 cm travel transverse linear stages
- Three manual vertical stages
- Two rotary stages
- Ti tubing installed inside Al beam chamber as guide for carbon fiber Hall probe assembly

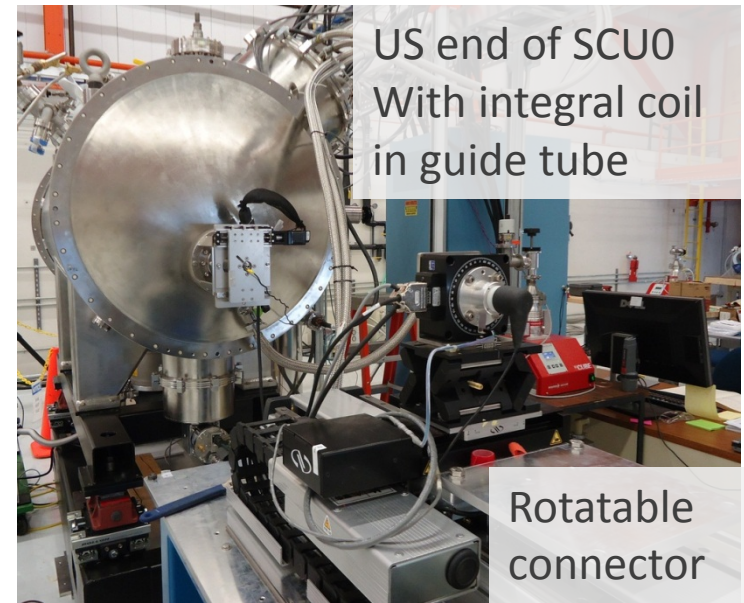


SCU Horizontal Magnetic Measurement System



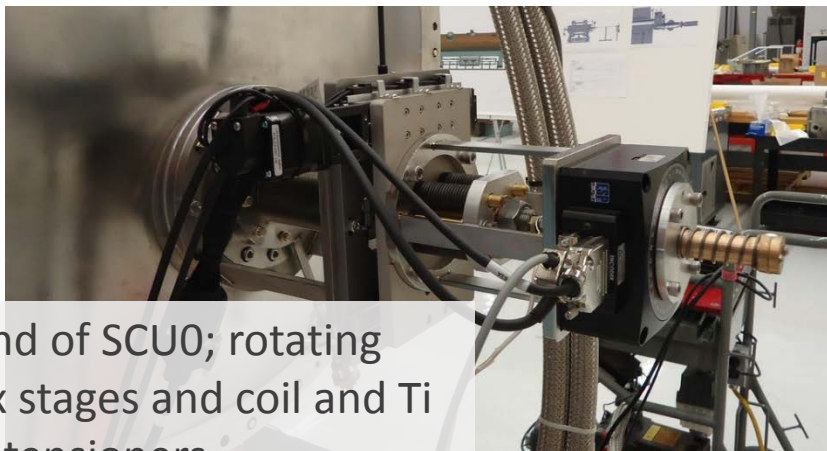
US end of SCU

3.5 m linear stage

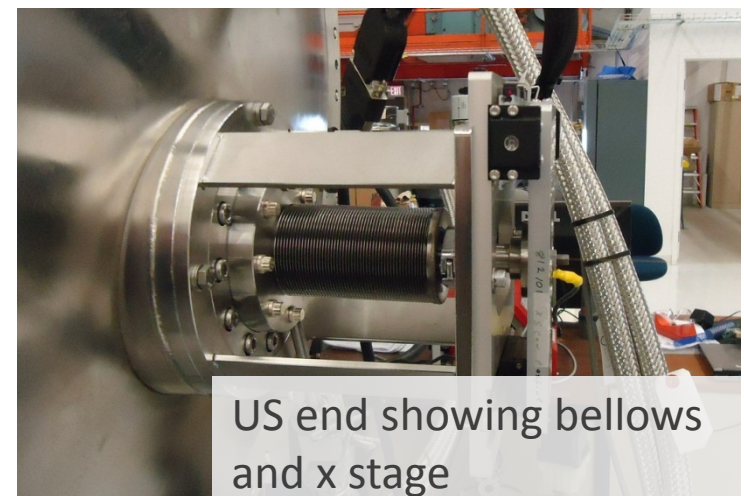


US end of SCU
With integral coil
in guide tube

Rotatable
connector



DS end of SCU; rotating
and x stages and coil and Ti
tube tensioners



US end showing bellows
and x stage

Custom 3-sensor Hall probe assembly

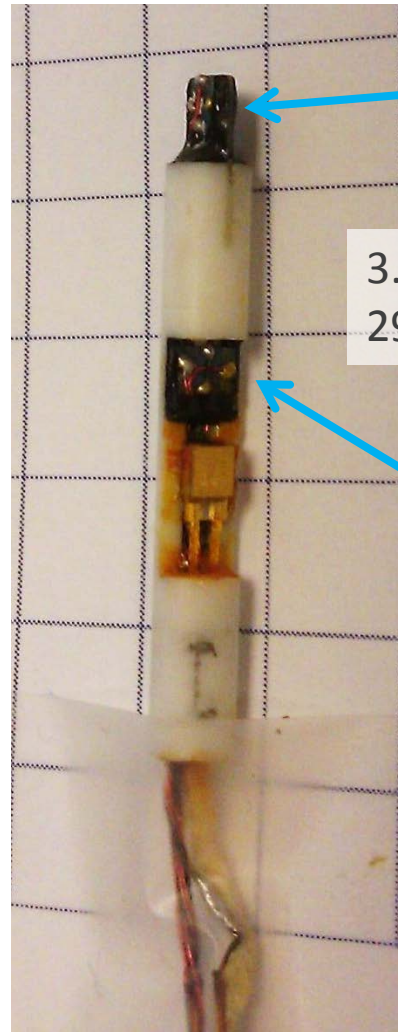
Three Arepoc Hall sensors and one temperature sensor mounted to a ceramic holder which is then installed in a carbon fiber tube

Two sensors measure B_y above and below the mid-plane separated by $\sim 1\text{mm}$ (suggested by I. Vasserman) [3]

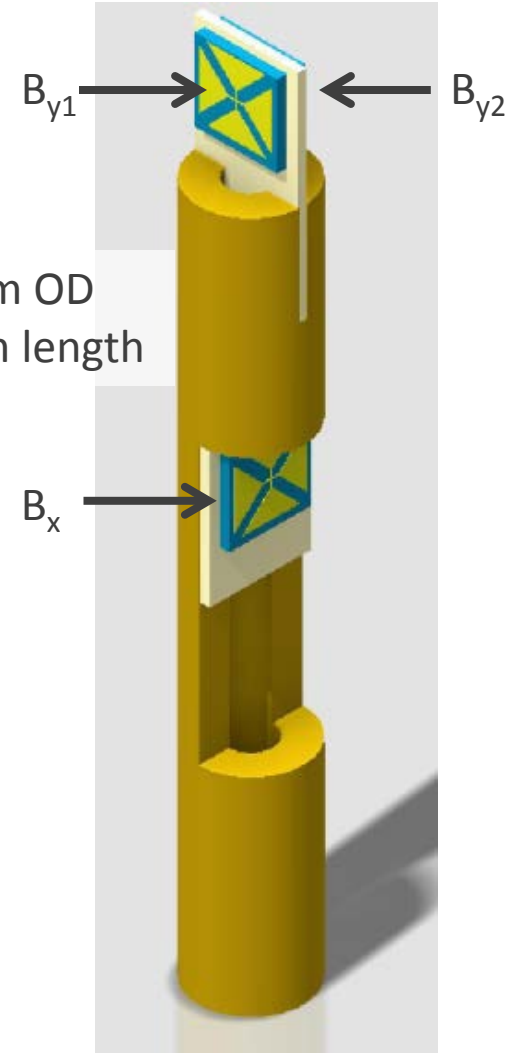
These sensors were calibrated by M. Abliz [11]

Third sensor measures B_x

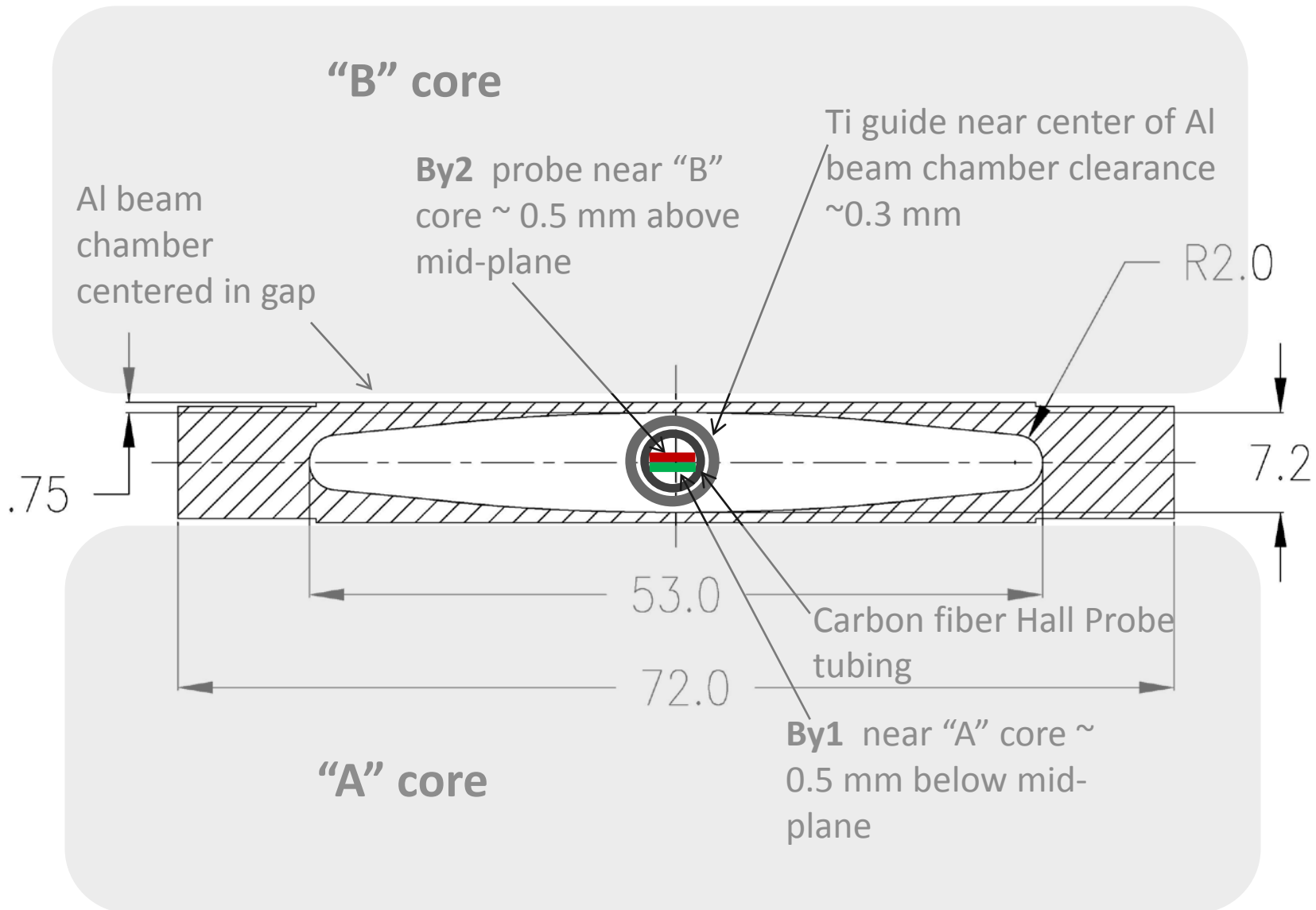
Nominal K1 scale factor 14 T/V



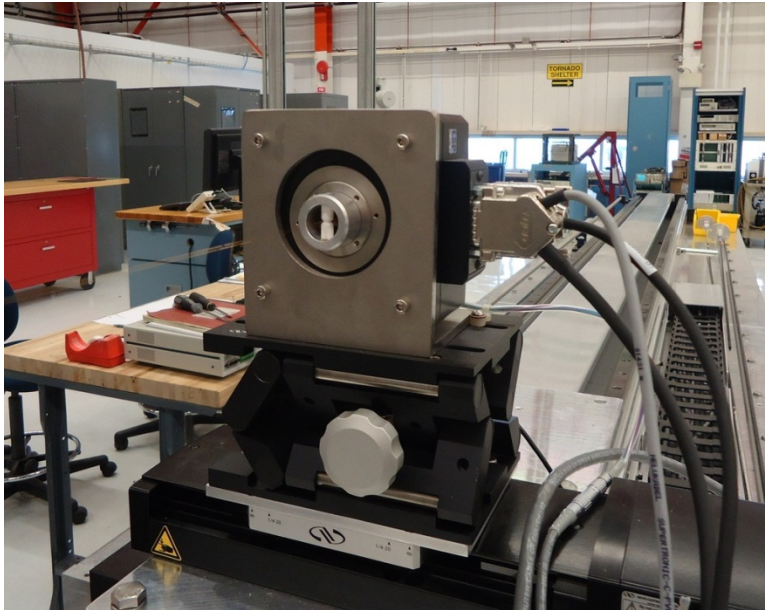
3.8 mm OD
29 mm length



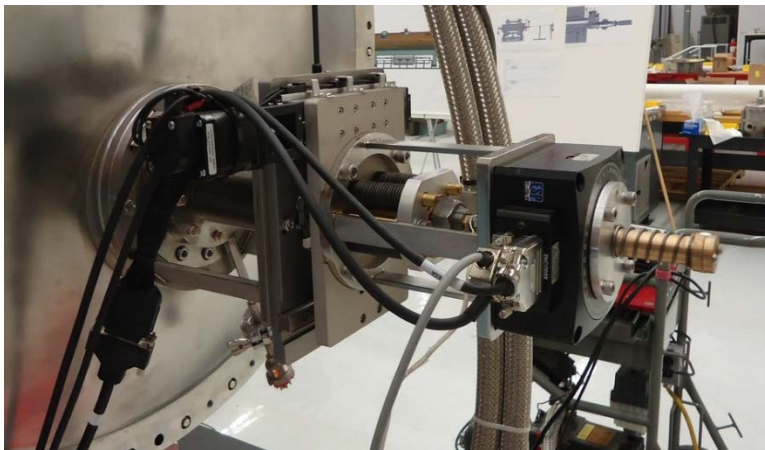
Al beam chamber with Ti guide tube and CF Hall probe



SCU Integral coil system



Upstream end rotating stage with ceramic pin to define coil width and position

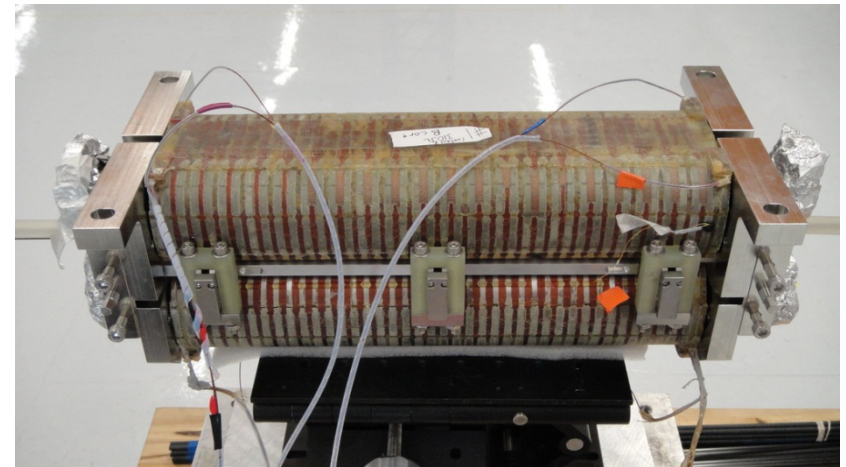


Down-stream end rotating stage with ceramic pin and brass tensioning fixture

One turn integral coil is supported at each end by ceramic pins with 4 mm V cut mounted to rotating stages
Coil can be configured at rectangular, delta or figure 8

Review of SCU0 basic design

- SCU0 consists of two 42 pole SC magnet cores with a 9.5 mm gap between cores.
- Each core wound with a continuous SC for the 41 main coils
- 11 turn correction coils are wound on last two main coils of each end of the cores
- One main power supply energizes the main coils in series
- One, or two corrector supplies may be used to energize all corrector coils, or up-stream and down-stream independently
- The ideal correction current is a function of the main current, and for lowest phase errors should be equal on both ends of the device
- Adjustment of the correction coil current affects the average photon beam angle (average value of the 1st field integral), but has very little effect on the e-beam exit angle (final 1st field integral) [6,7,8,9]



ID Field error limits from APS Upgrade PDR 8/22/2012

Table 4.4-6: Effect from ID errors.

Name	Expression	Beam effect
First field integral	$I_{1x,y} = \int B_{y,x} ds$	Beam position
Second field integral	$I_{2x,y} = \int \int B_{y,x} ds' ds$	Beam position
Quadrupole integral	$\int (dB_y/dx) ds$	Tune
Skew quadrupole integral	$\int (dB_x/dx) ds$	Vertical beam size
Higher-order multipole integrals	$\int (d^n B_y/dx^n) ds,$ $\int (d^n B_x/dx^n) ds$	Dynamic aperture, lifetime

Table 4.4-7: ID error tolerance specification in 1995.

(a) Steering		(b) Multipole		
Order	Limit ^a	Order	Normal Component $B_0 L b_n$ ^a	Skew component $B_0 L a_n$ ^a
I_{1x}	100 G-cm	1	50 G	50 G
I_{1y}	50 G-cm	2	200 G/cm	100 G/cm
$I_{2x,y}$	1×10^5 G-cm ²	3	300 G/cm ²	500 G/cm ²

^a Superseded by recent study (Tables 4.4-8 and 4.4-9).

^a $\int (B_y + iB_x) dl = B_0 L \sum_{n=0}^{\infty} (b_n + ia_n)(x + iy)^n$

Table 4.4-9: Requirements for absolute first- and second-field integral errors based on local orbit modeling with x-ray BPMs participating in orbit correction [4.4-25].

Table 4.4-8: Undulator field integral rate-of-change limit requirements [4.4-25].

Field integral	Limit for a 5-second duration ramp	Unrestricted in duration	Driving requirement
Rate of $\int B_y dz$	21 G-cm/s	5.0 G-cm/s	horizontal orbit stability
Rate of $\int B_x dz$	16 G-cm/s	4.0 G-cm/s	vertical orbit stability
Rate of $\int dz \int B_y dz'$	43,000 G-cm ² /s	10,000 G-cm ² /s	horizontal orbit stability
Rate of $\int dz \int B_x dz'$	4900 G-cm ² /s	1200 G-cm ² /s	vertical orbit stability

Field integral	Single 5-m device	One 2.5-m device upstream or downstream	Two independent 2.5-m devices ¹
$\int B_y dz$ (G-cm)	900	80	60
$\int B_x dz$ (G-cm)	90	25	18
$\int dz \int B_y dz'$ (G-cm ²)	120,000	10,000	7,000
$\int dz \int B_x dz'$ (G-cm ²)	12,000	3,200	2,300

¹ The two undulators are uncorrelated, so we made the tolerance $\sqrt{2}$ tighter than for a single ID.



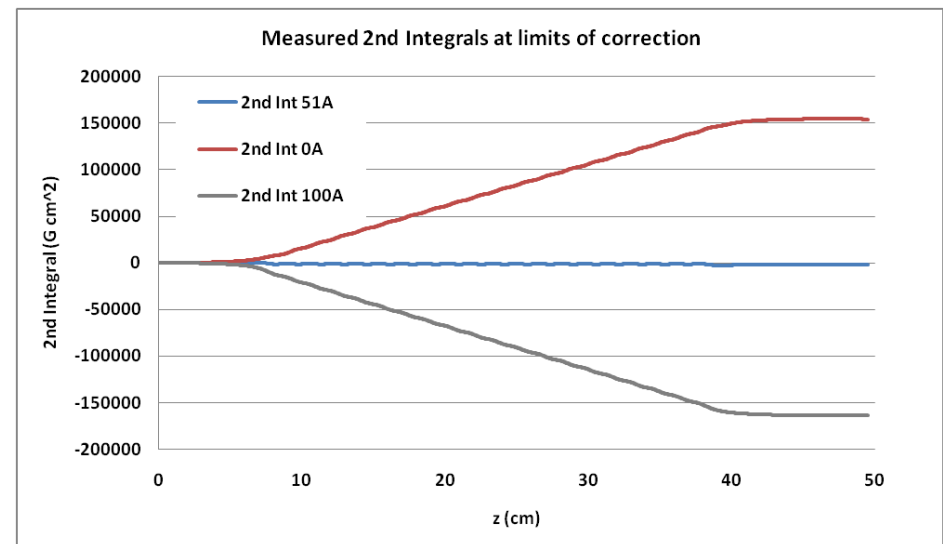
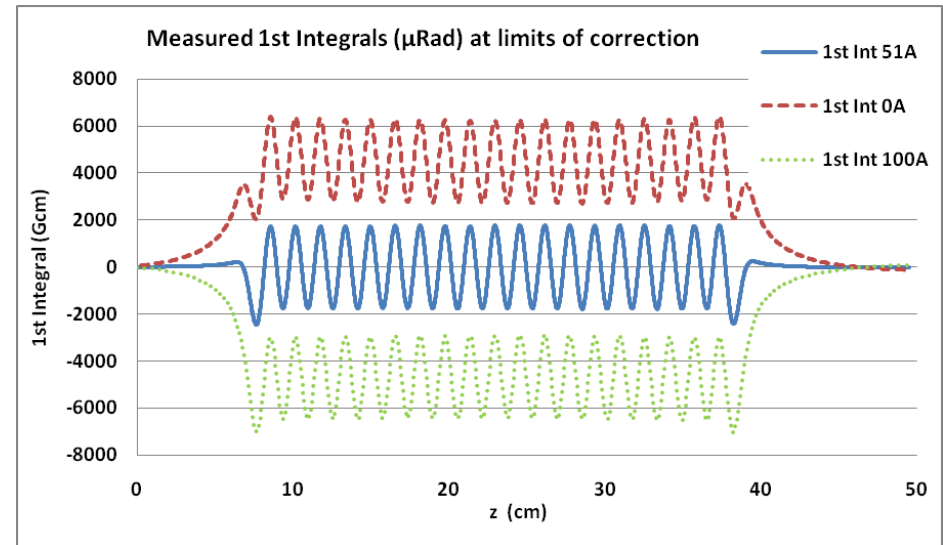
Range of correction with main current at 500 A [10]

The plot to the right shows typical 1st field integrals with maximum, minimum and ideal correction current with 500 A main current

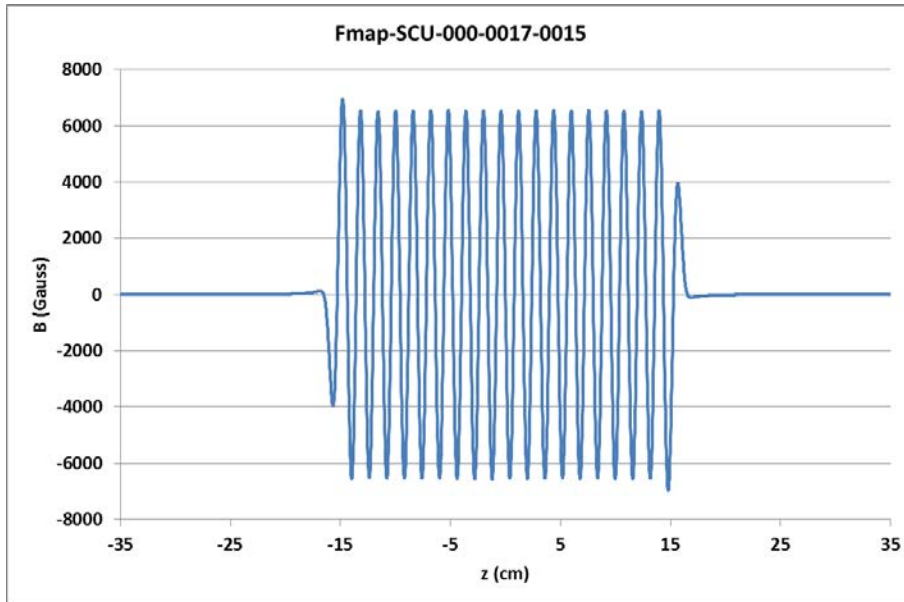
5000 G-cm \sim 200 μ Rad angle @ 7GeV

The average photon beam angle can be adjusted ± 200 μ Rad relative to the incoming e-beam

The plot to the right shows the range of the 2nd field Integrals, e-beam offset range at exit $\sim \pm 70$ μ m

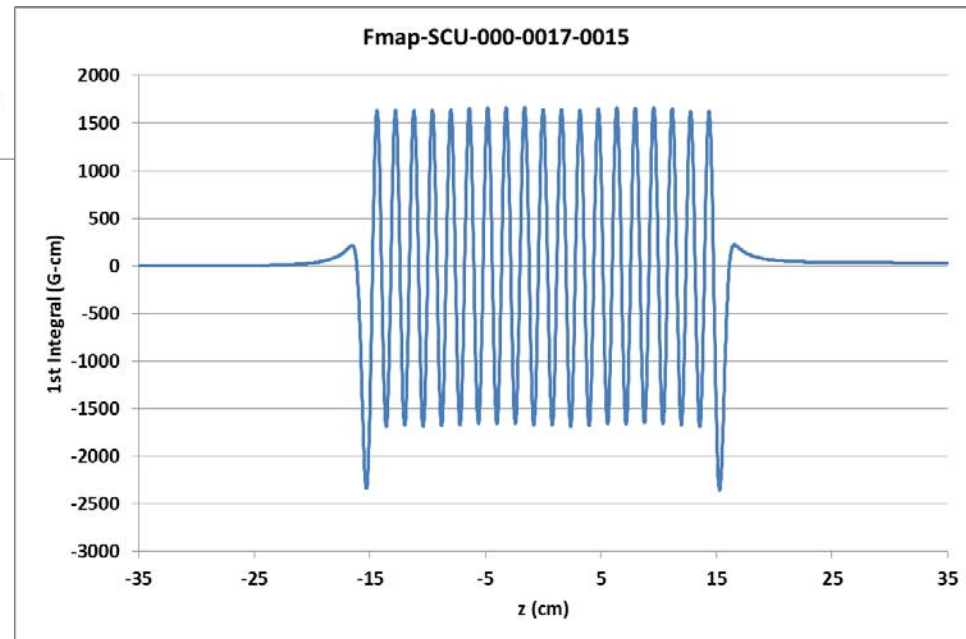


Typical Hall Probe measurement results at 500 A



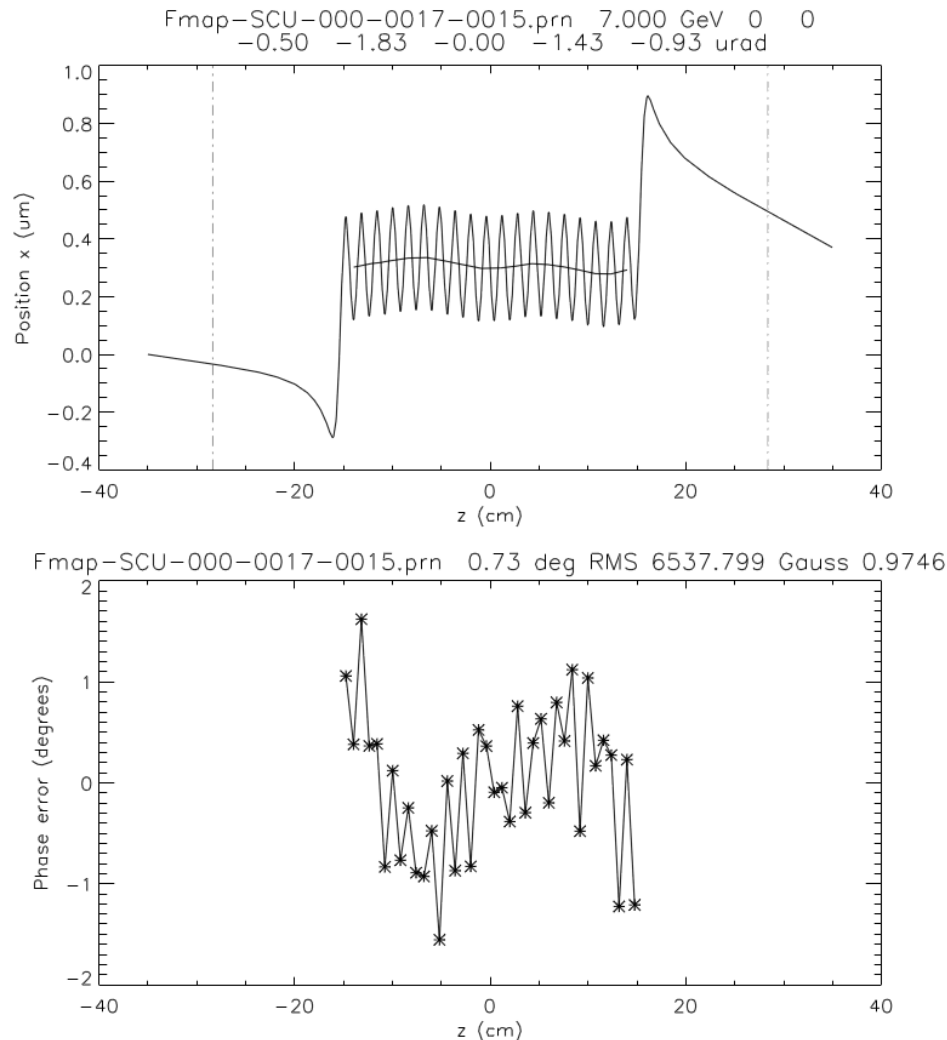
Typical B_y field with Main coil current of 500A and correction current of 51.7A

1st field integral of above data

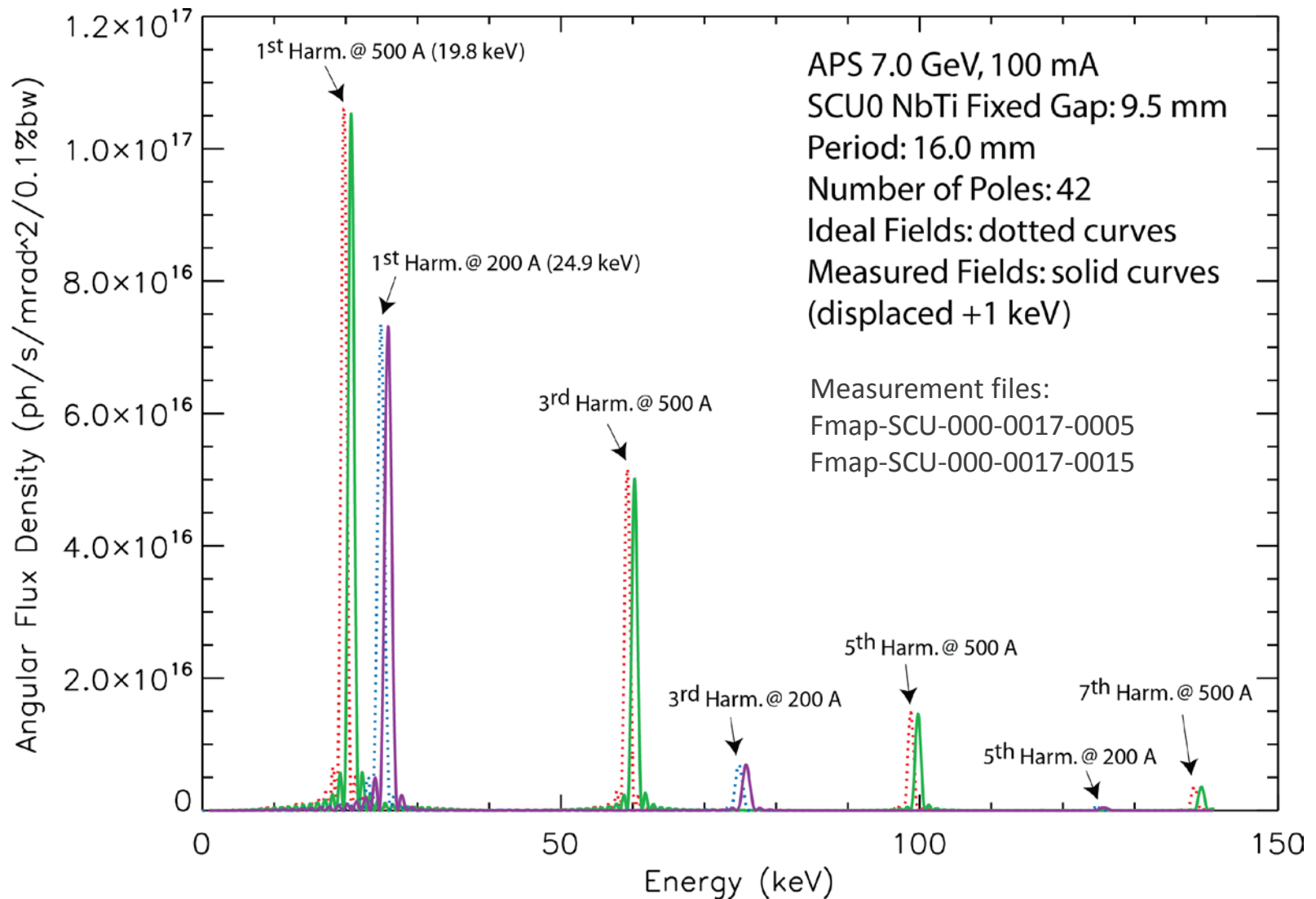


SCU0 Trajectory and phase errors

Main current 500A corrector current 51.6A



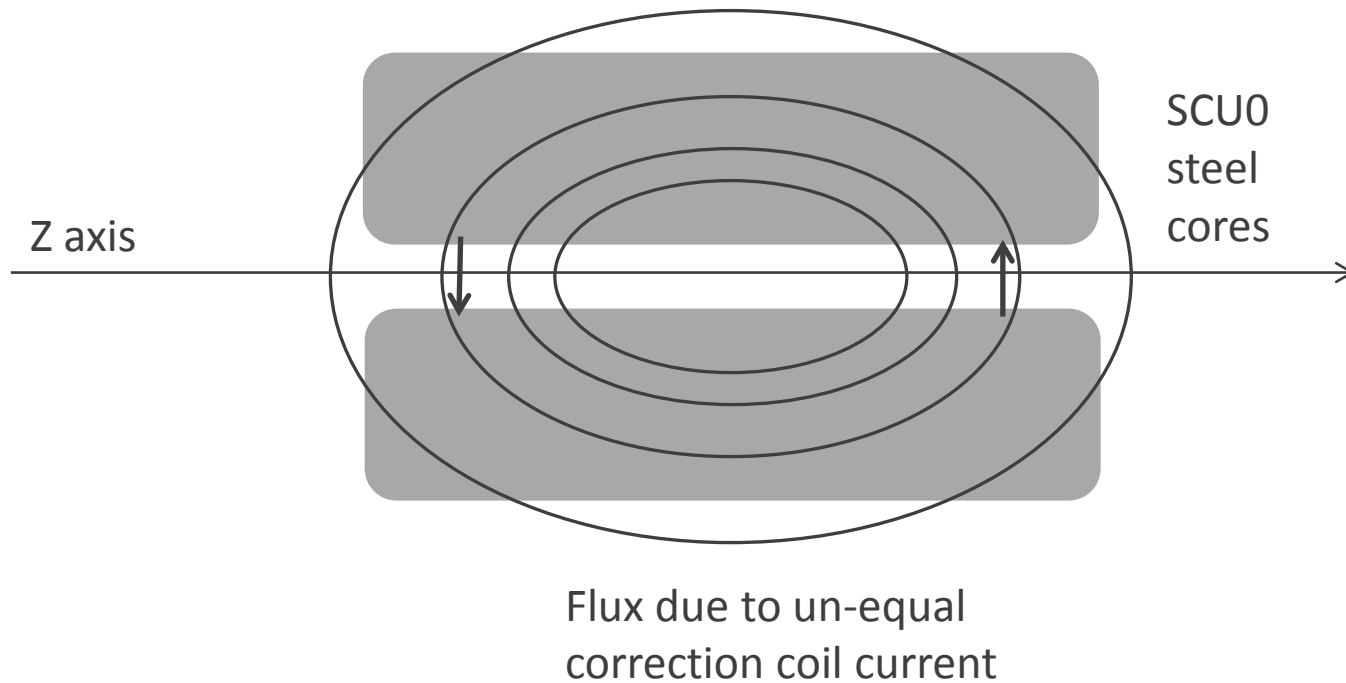
SCU0 Spectral plots calculated by R. Dejus



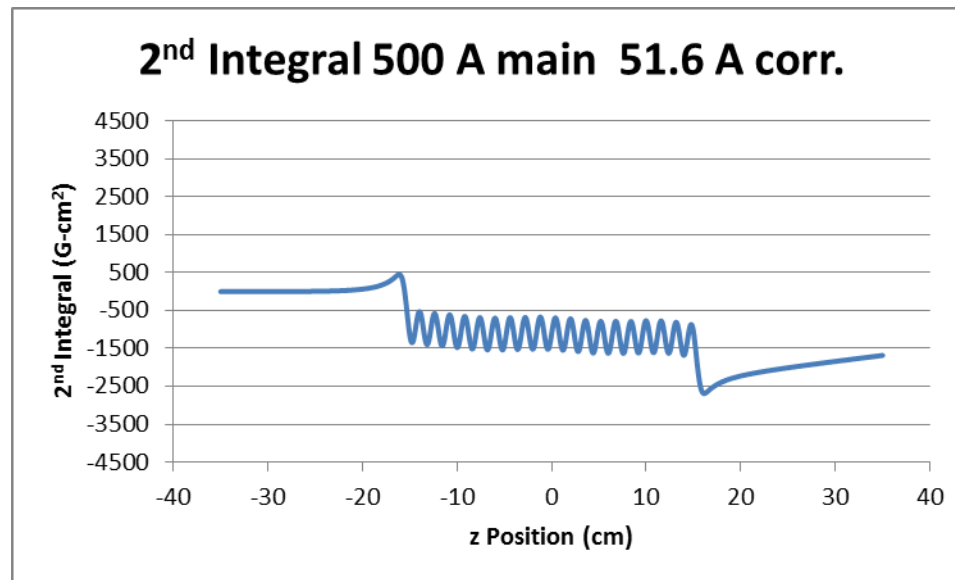
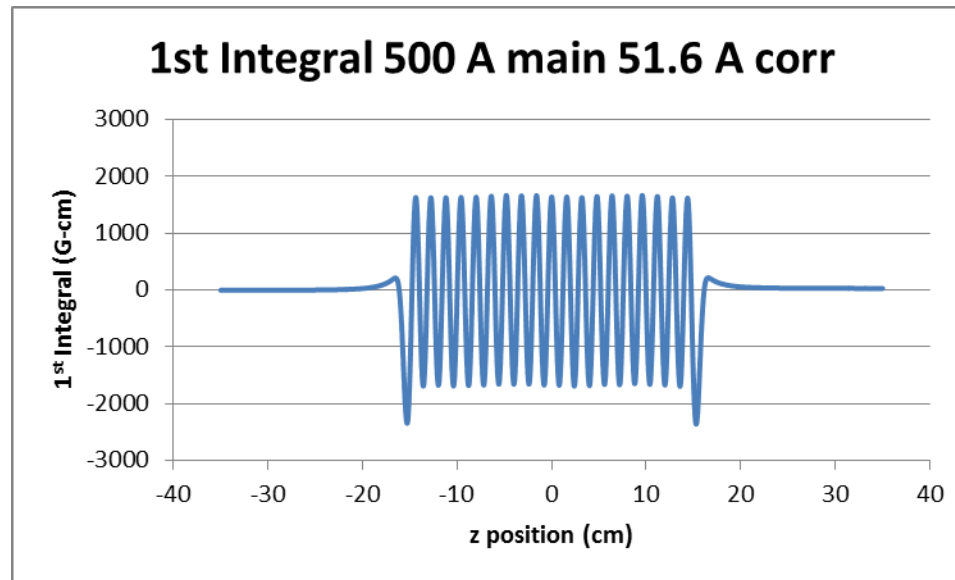
Effects of differential correction coil currents

- By design, under normal circumstances, the four SCU0 correction coils should be energized with equal currents. If unequal currents are used on the upstream and down-stream ends, flux will be generated in the body of the steel cores.
- The plots on the next slide show the effects of energizing the up-stream and down-stream correction coils with unequal currents. For plots labeled +5 A diff, the US end correction coil was energized to 56.6 A and the DS end to 46.7 A. For plots labeled -5 A diff, the currents were swapped.
- When the correction coils are energized unequally, flux is generated in the steel cores and produces a vertical field which varies along the length of the magnet structure with the largest field near the ends. The polarity of the vertical field changes on either end of the magnet center.
- This vertical field causes the trajectory of the e-beam to curve horizontally with a constantly changing angle while inside the body of the SCU.
- This curved trajectory destroys the symmetry of the device and for a 10 A difference in correction current (with the main at 500 A) the phase errors become close to 10 degrees rms.
- Ideally symmetrical correction current should be used unless there is some need to increase the phase errors or widen the photon angular distribution

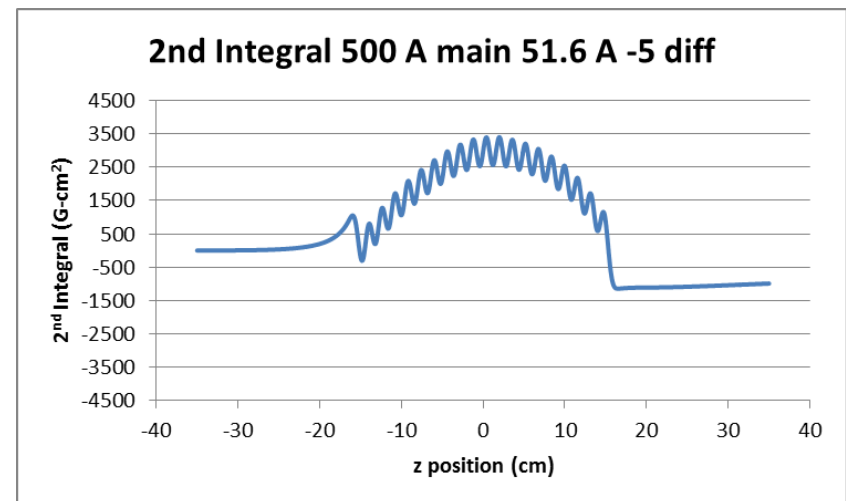
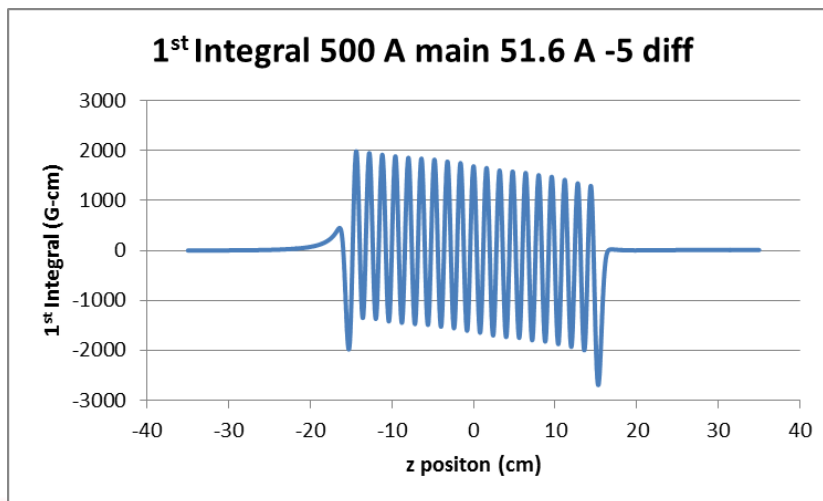
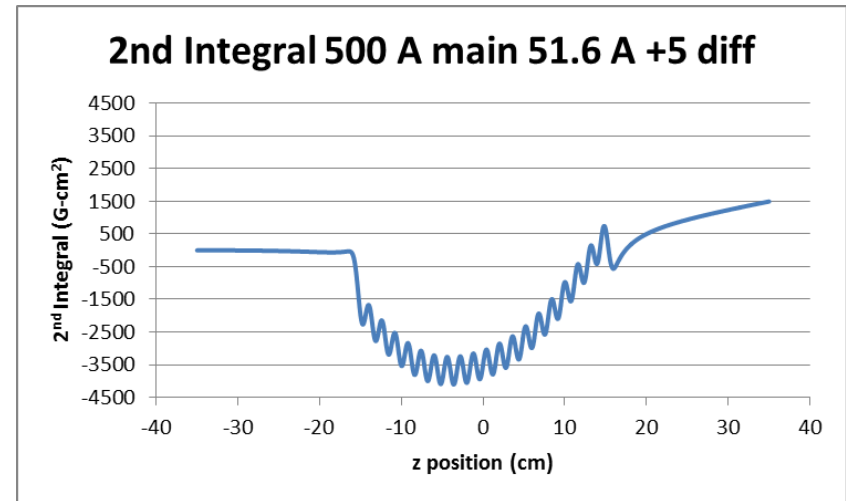
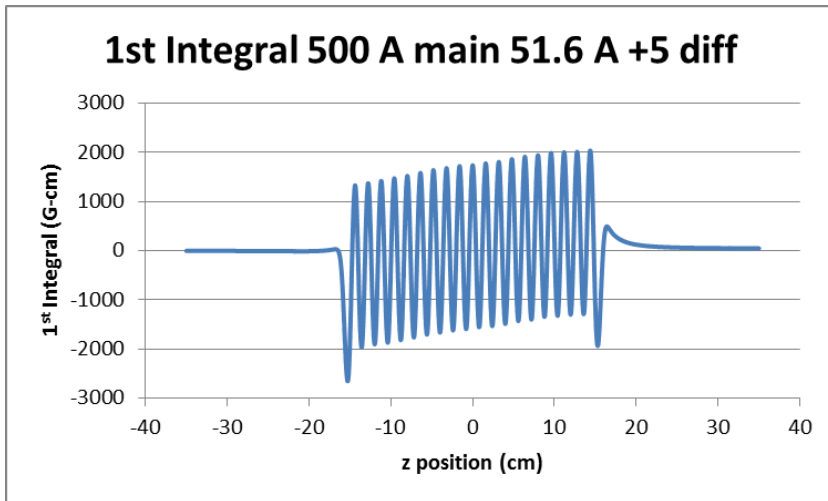
Flux paths due to un-equal correction coil currents



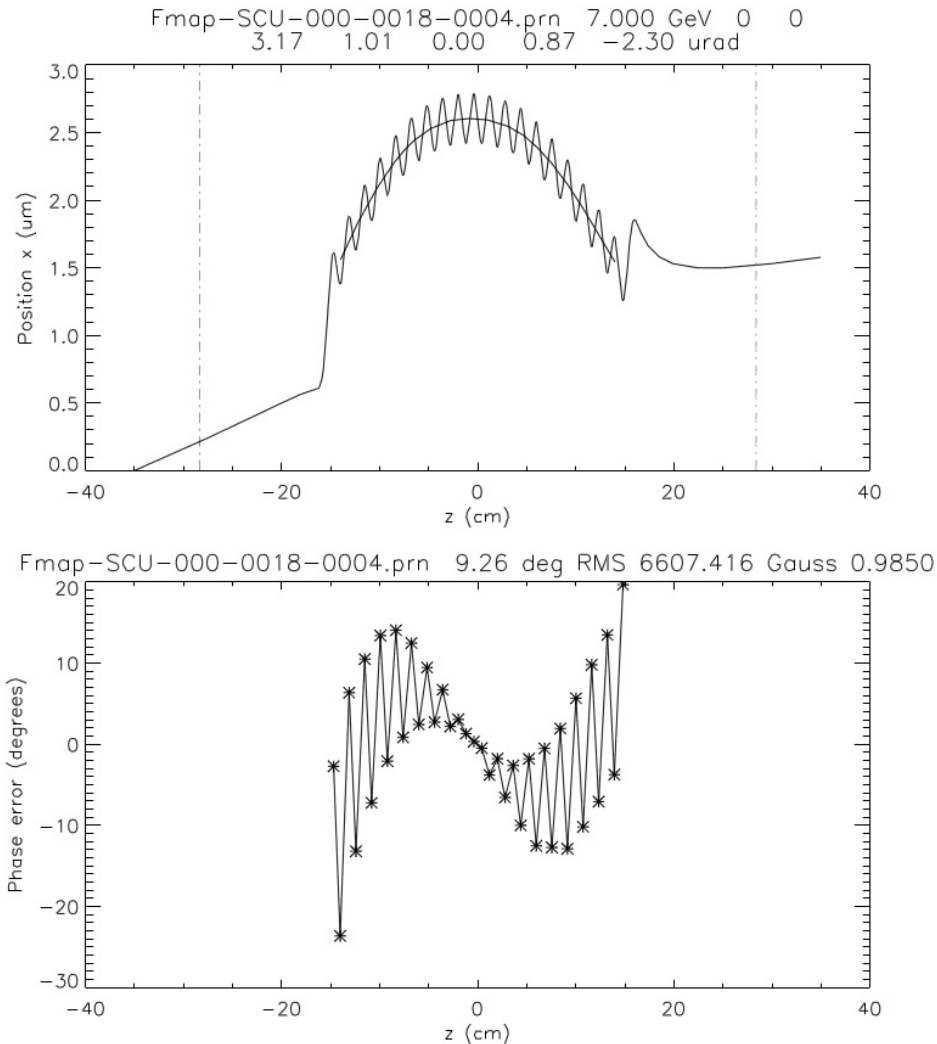
2nd Integral with equal correction coil currents



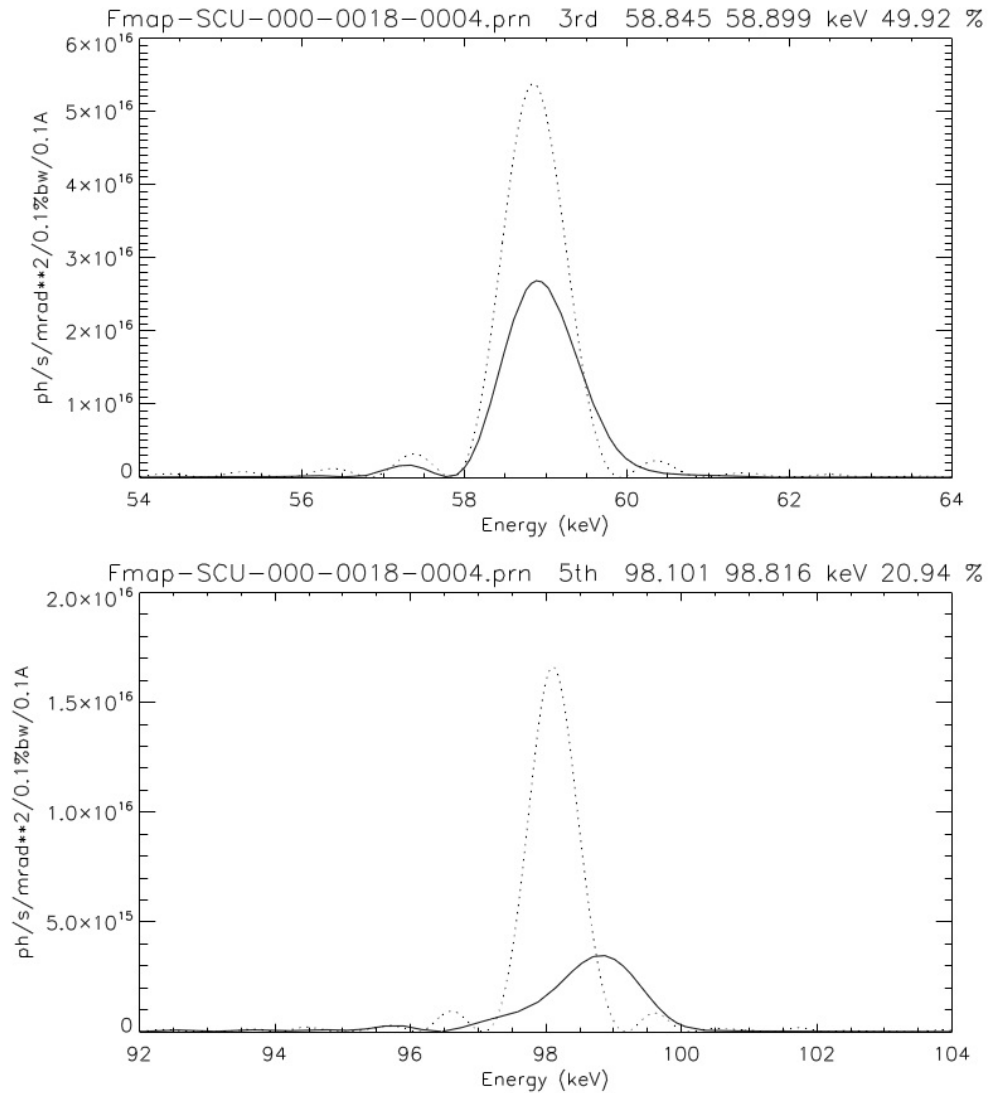
1st and 2nd Integrals with average corrector current of 51.6 A, with difference of ± 5 A between ends



Trajectory and Phase errors for 5 A differential corrector current



3rd and 5th harmonics for 5 A differential corrector current



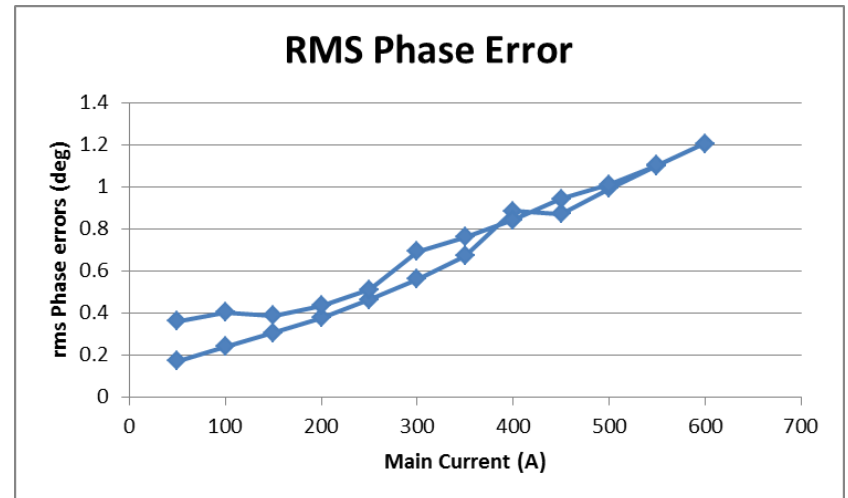
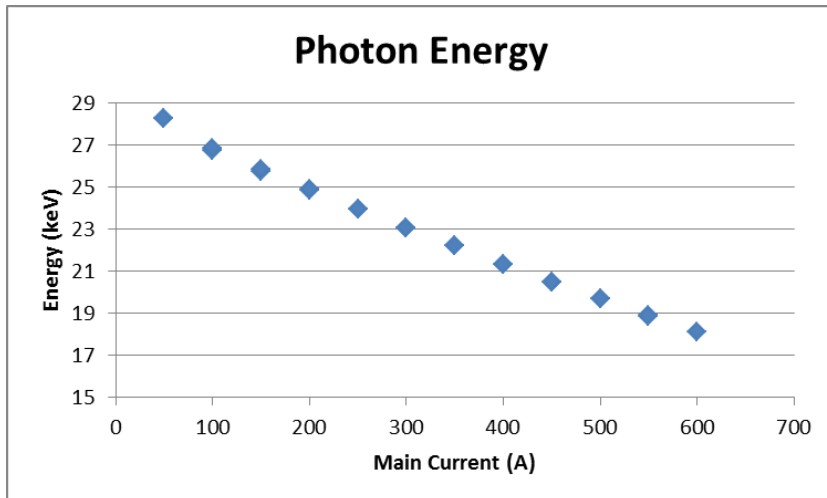
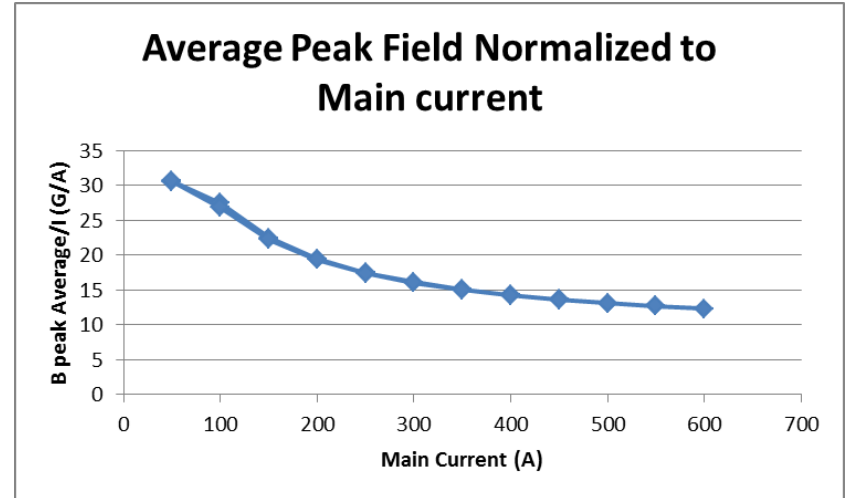
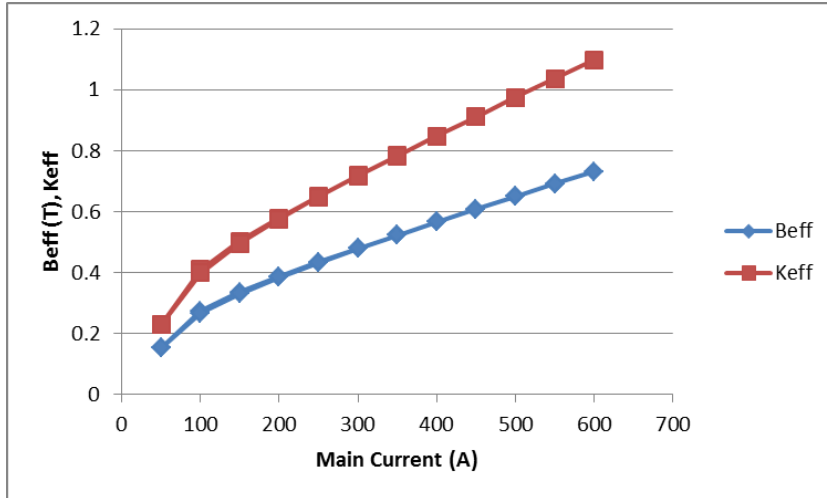
Hall probe excitation data

- The following current-dependent plots show the results of Hall probe measurements done after conditioning the magnet 4 times from 0 to 600 A then performing measurements at 50 A increments up to 600 A and back to 0A.
- The change in probe temperature was typically 1 Kelvin over the span of 70 cm during the measurement. This introduces a slight change in gain and offset to the Hall voltage so the calculation of the 1st and 2nd integrals and phase errors show some small non-repeatable behavior.
- For these measurements an averaged lookup table for the correction current was used. The lookup table values were experimentally derived from Hall probe measurements.
- It can be noted that the largest change due to the current loop was in the 2nd field integral near 200 A. The average photon beam angle would be within a range of ± 3 μ Rad without any feedback or manual correction if the average lookup table is used.
- The average trajectory angle sensitivity to correction current is ~ 4 μ Rad/A

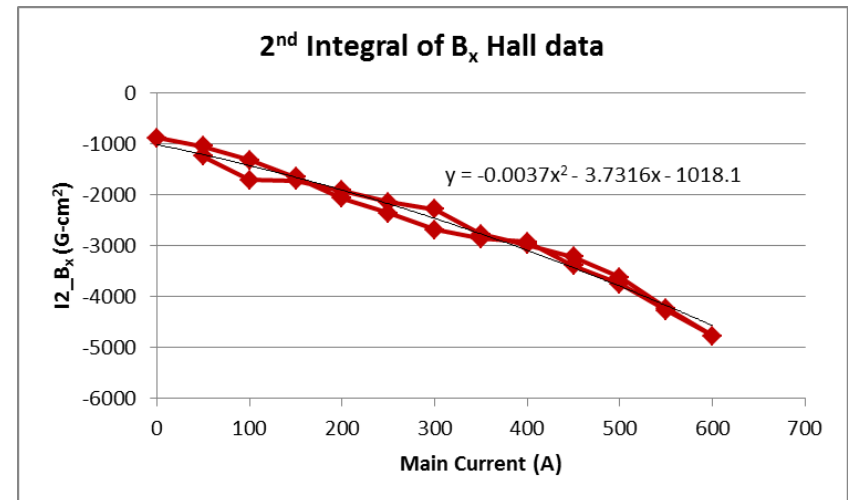
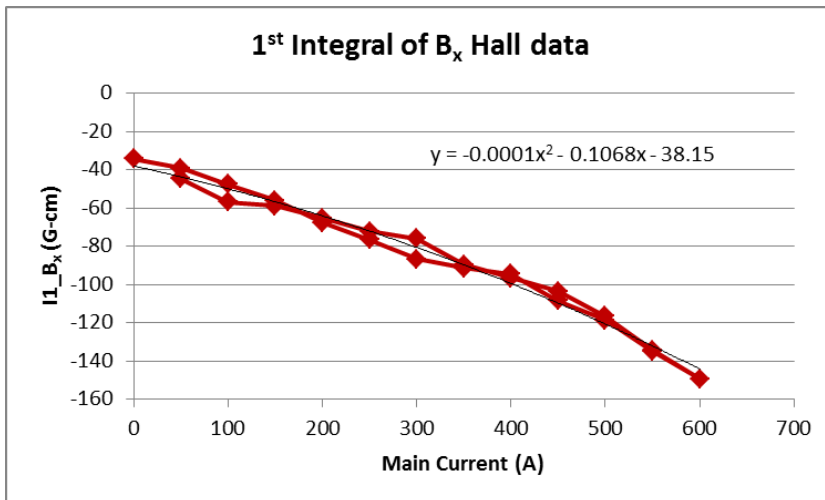
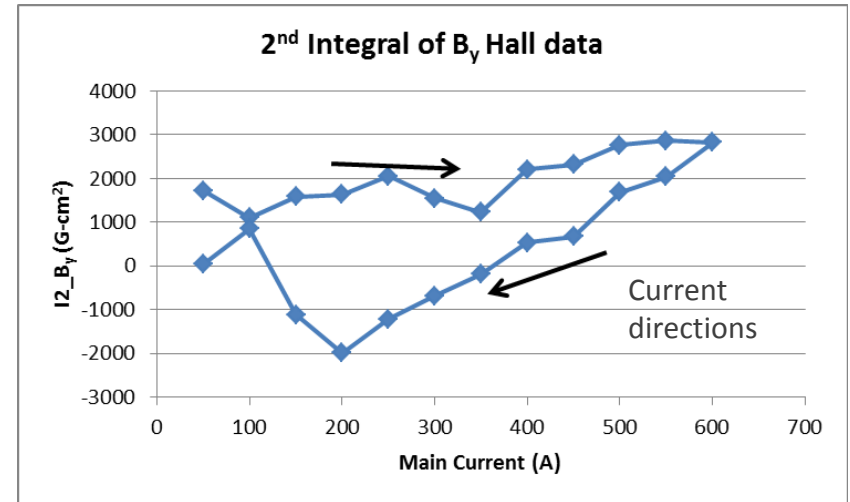
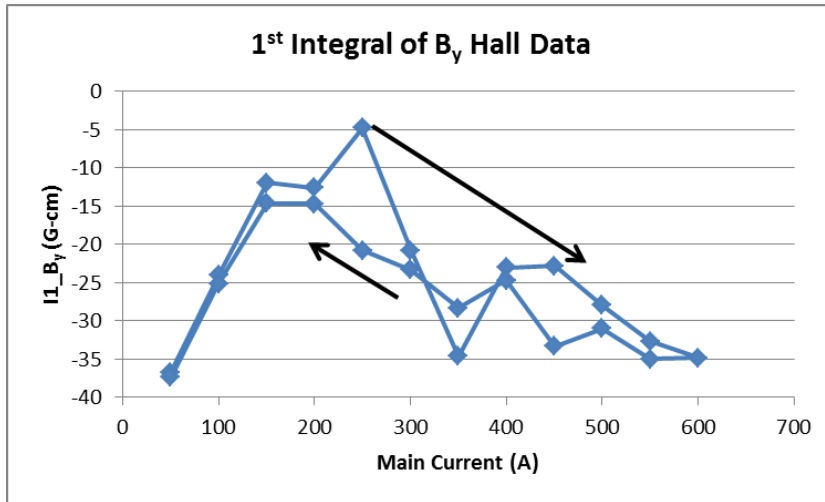


Some Current dependent parameters based on Hall probe measurements

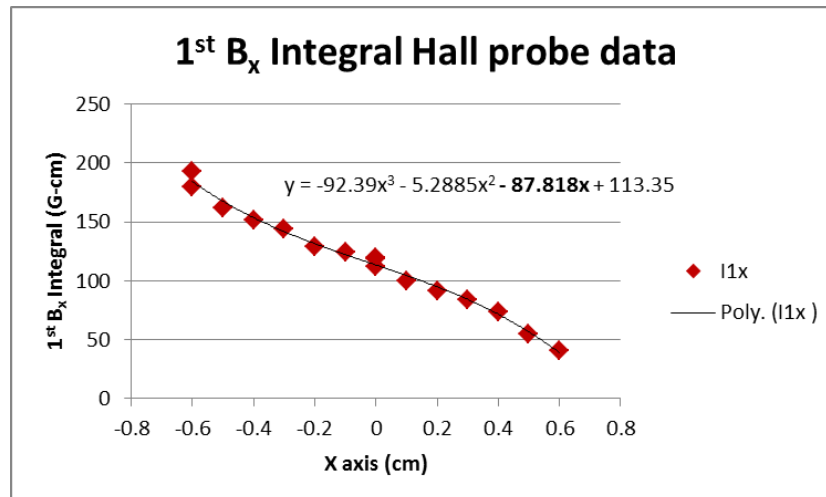
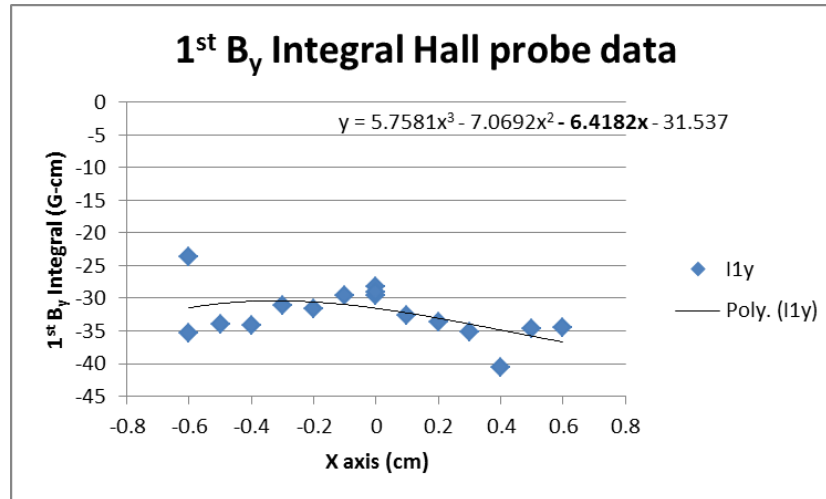
Fmap-SCU-000-0017-0002 to 0024



1st and 2nd field integral as function of current based on Hall probe measurements

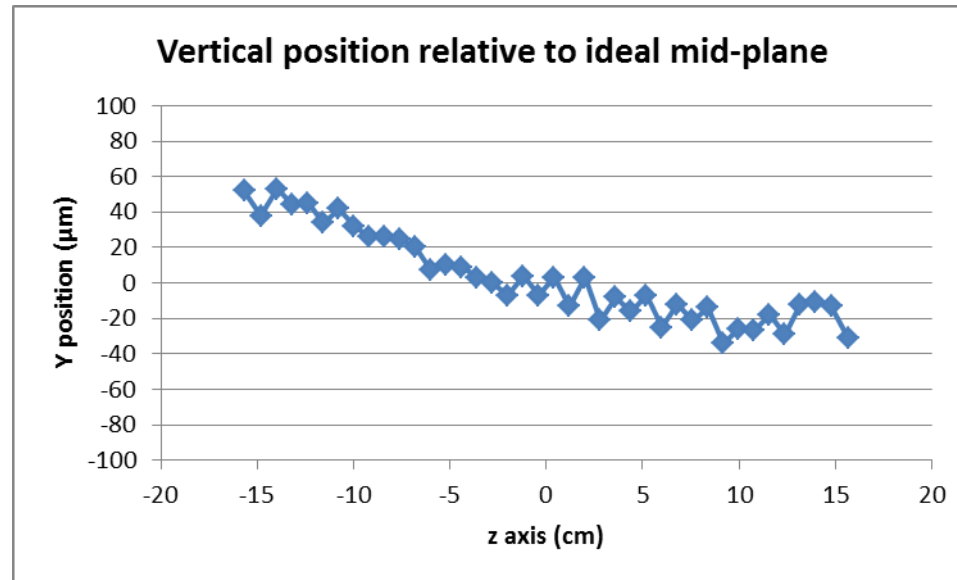


1st Integrals of B_y and B_x as a function of x position main I = 500 A and correction I = 51.5A



Calculated Integrated skew quadrupole component ~ 90 G

Vertical position of Hall probe center relative to the ideal magnetic mid-plane



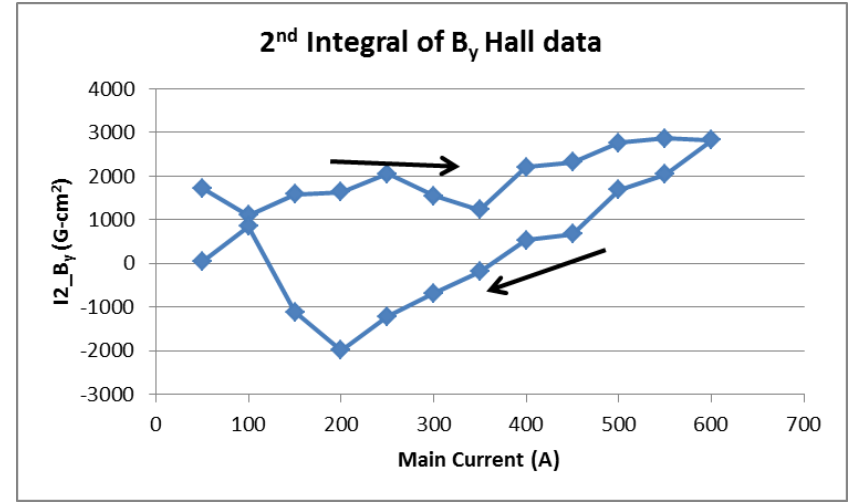
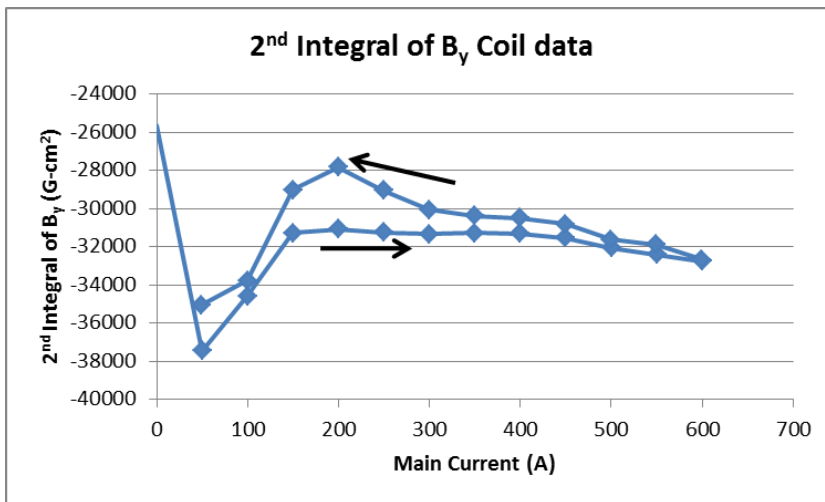
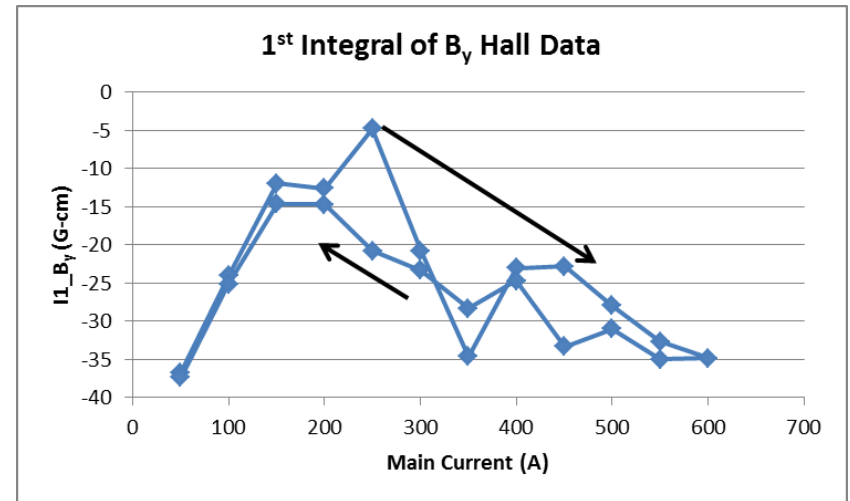
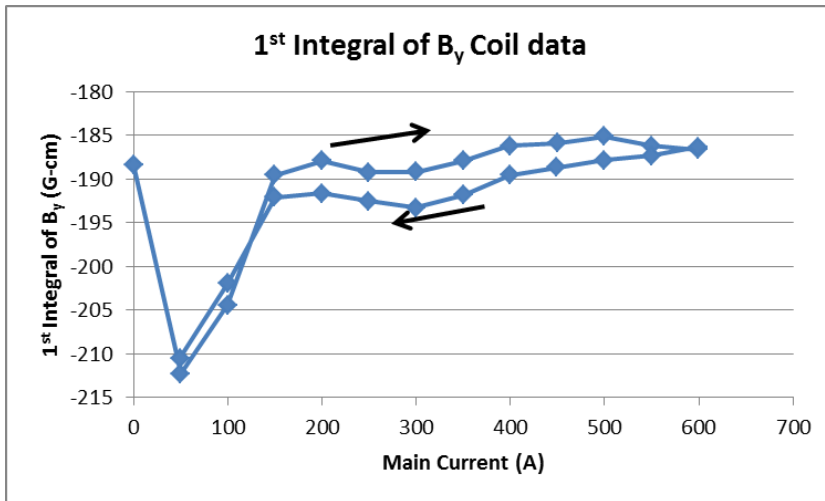
This plot shows the calculated Hall probe average vertical positions (at the field peaks) relative to an ideal magnetic mid-plane assuming a hyperbolic cosine function for the vertical field. Details can be found in [1]

This shows the Hall probe path was very close to the magnetic center of the device, and the upstream end was about 60 μm higher than the center of the magnet. This was mostly due to an offset in the vacuum chamber end transition piece.

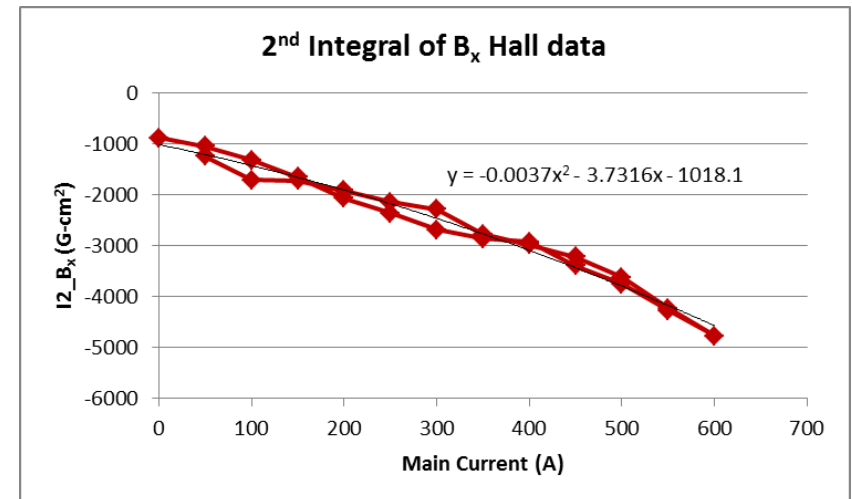
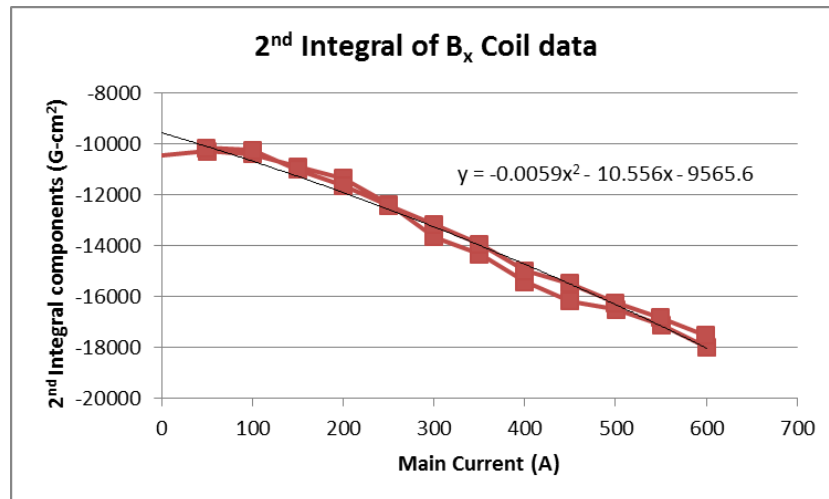
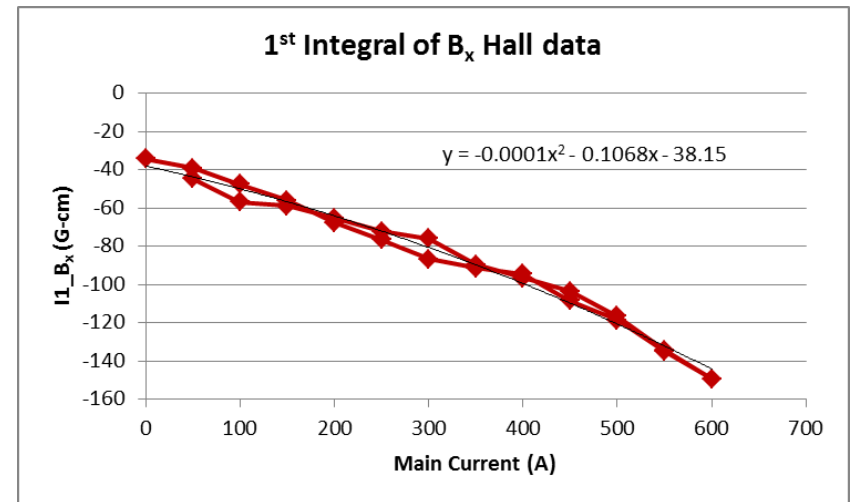
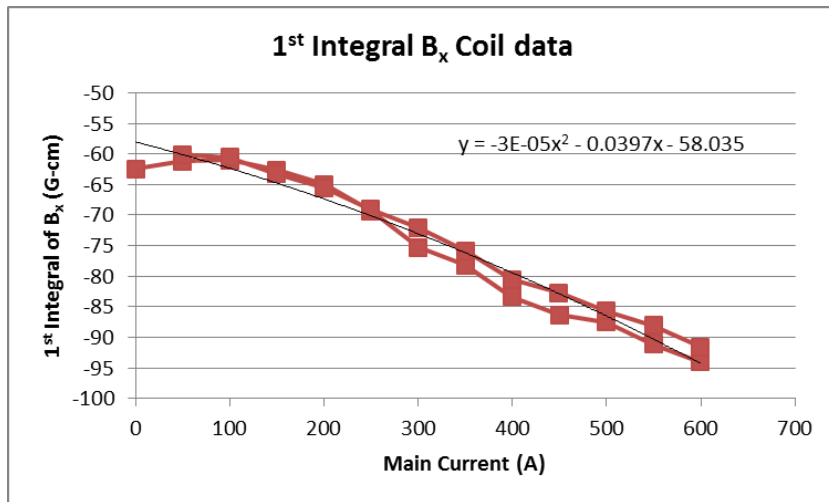
Rotating coil data

- Measurements were done to measure the 1st and 2nd field integrals as a function of current and horizontal position using a continuously rotating coil and a software based lock-in amplifier technique. [5]
- The SCU was first conditioned 4 times from 0 to 600 A then measurements were done from 0 to 600 A and back to 0 A at 50 A increments.
- The measured field integrals include the Earth's field which is the dominant component and is approximately 175 G-cm i.e. 0.5 G integrated over the 3.5 m coil length.

1st and 2nd B_y field integrals as a function of current

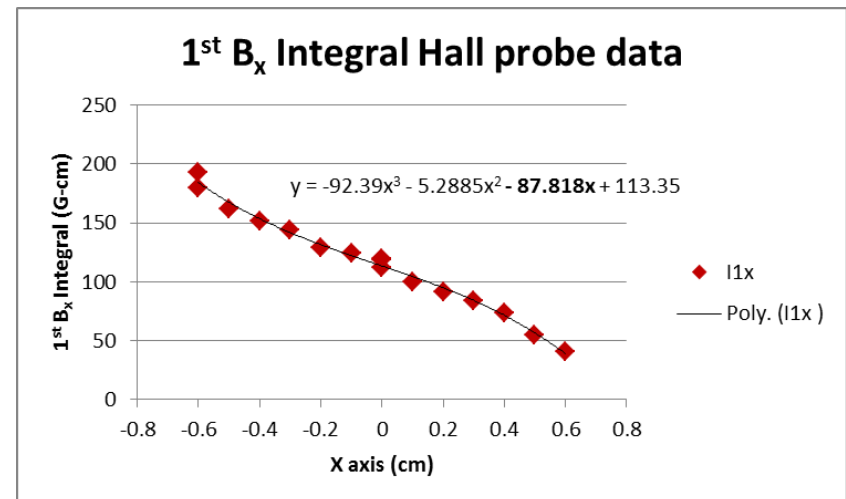
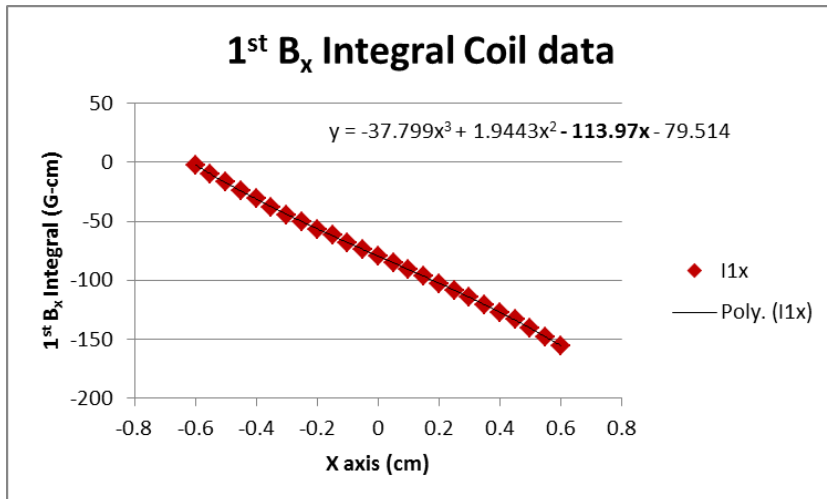
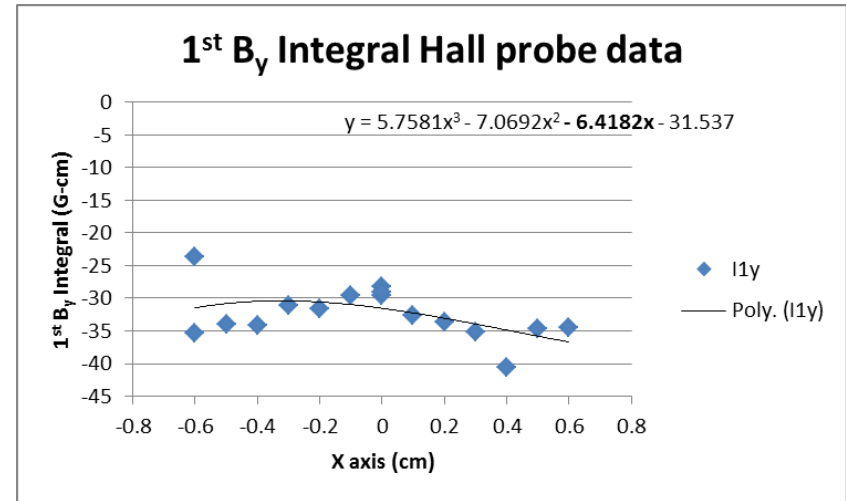
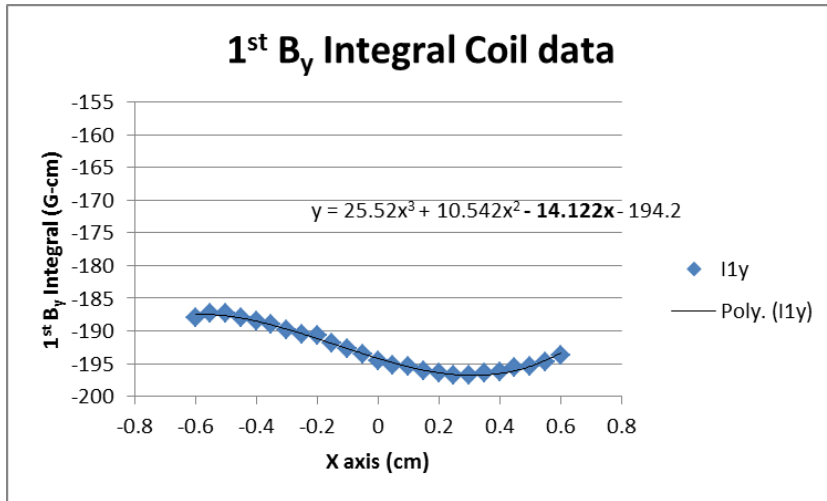


1st and 2nd B_x field integrals as a function of current

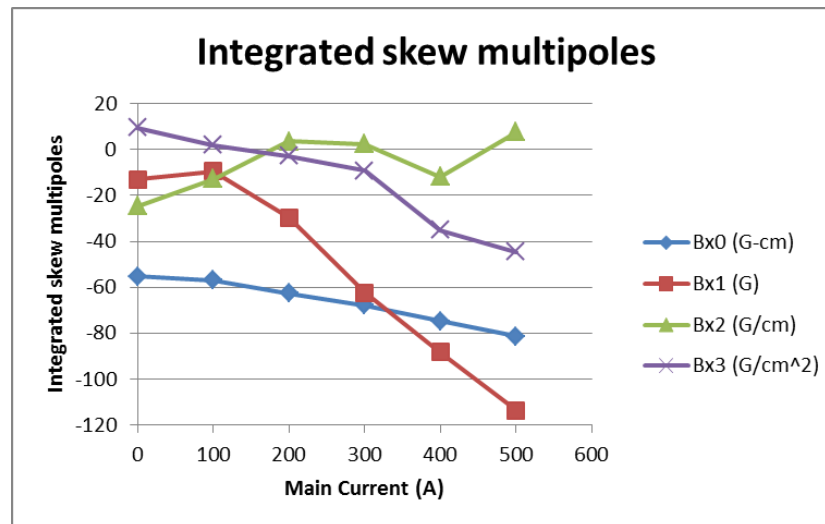
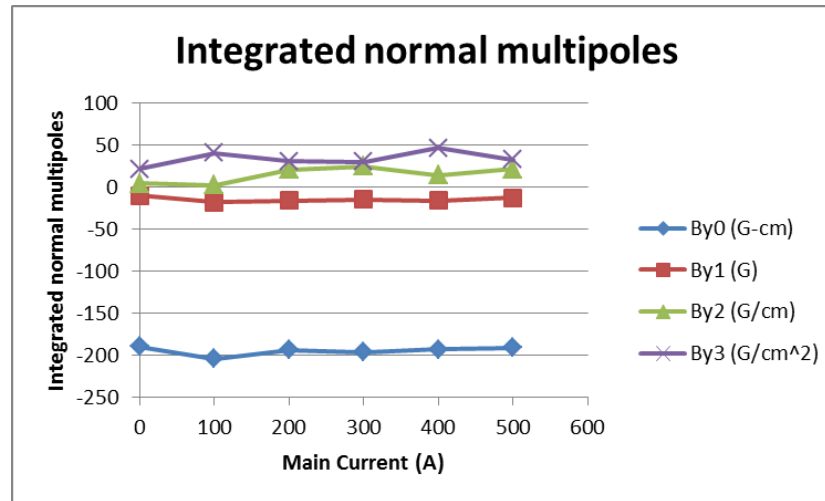


1st Integrals of B_y and B_x as function of x position

main I = 500 A and correction I = 51.5A



Integrated multipoles as function of main current from rotating coil data



Integrated B_y field during quench best case

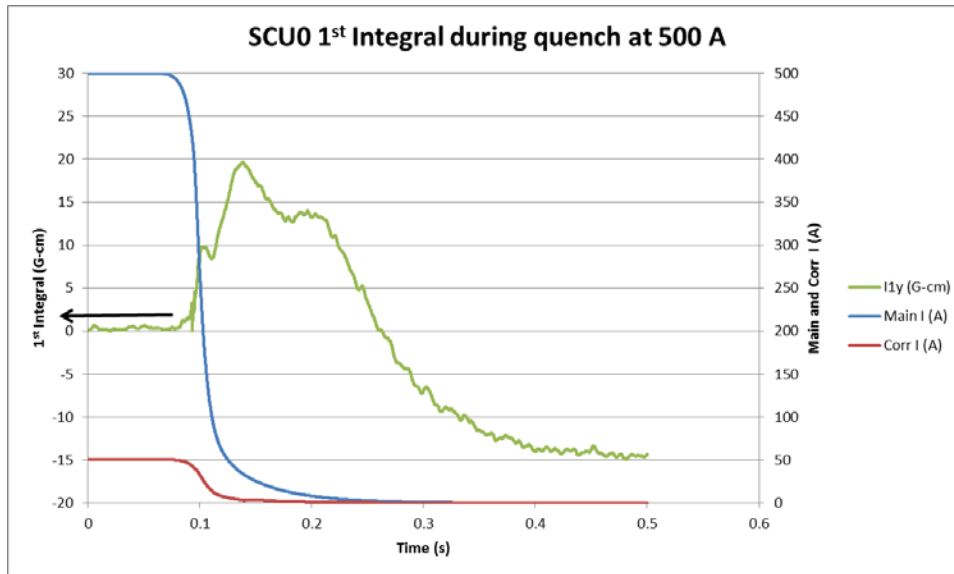
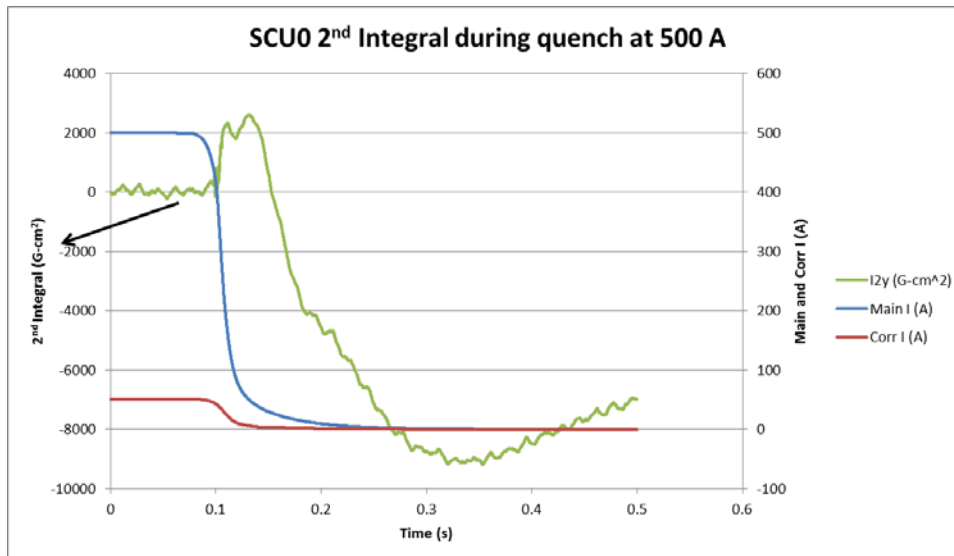


Table 4.5-8: Combined field errors during a quench, at fixed 9.5-mm gap.

Quantity	Specification
$B_x: \sqrt{I_1^2 + (I_2^2/\beta_0^2)}$	350 G-cm
$B_y: \sqrt{I_1^2 + (I_2^2/\beta_0^2)}$	2100 G-cm

Table 4.5-8 from APS Upgrade PDR

Heater induced quench
 Corrector current slaved to main current
 23 G-cm = 1 μ Rad
 2300 G-cm² = 1 μ m offset

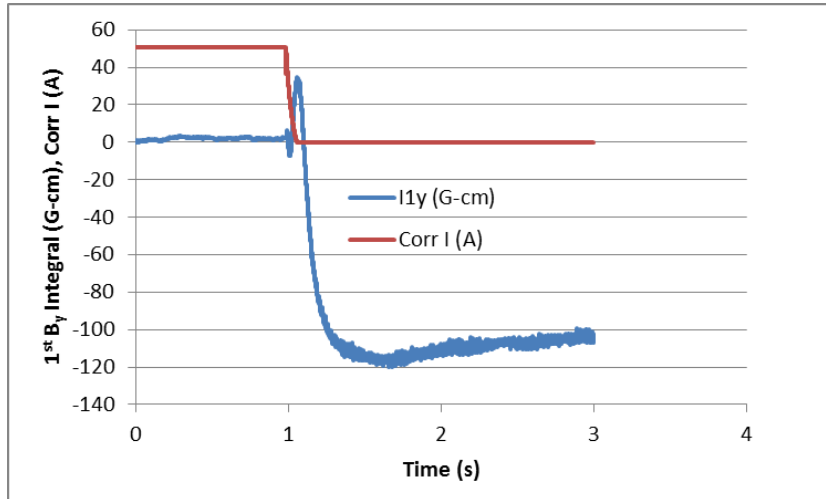


During a quench of the main coil, the corrector PS current will follow the main according to a lookup table. This will minimize disruption of the e-beam

Change of exit angle $\sim 1.5 \mu$ Rad in 50 ms
 Change of exit offset $\sim 4 \mu$ m

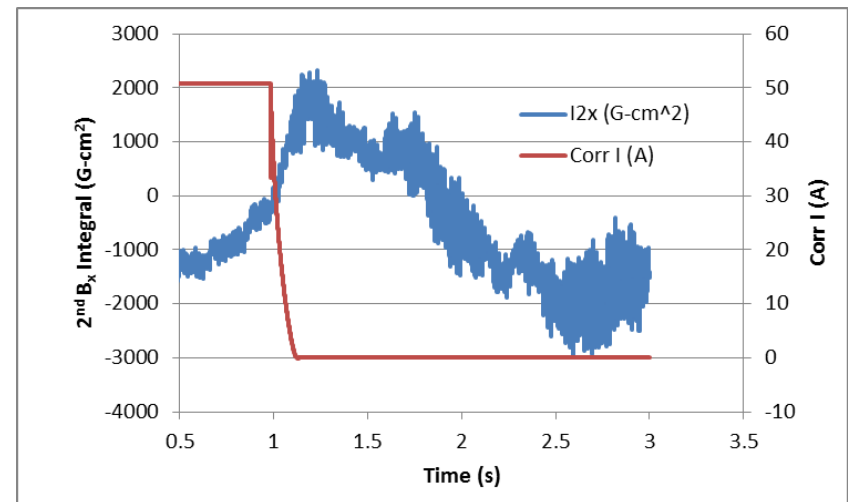
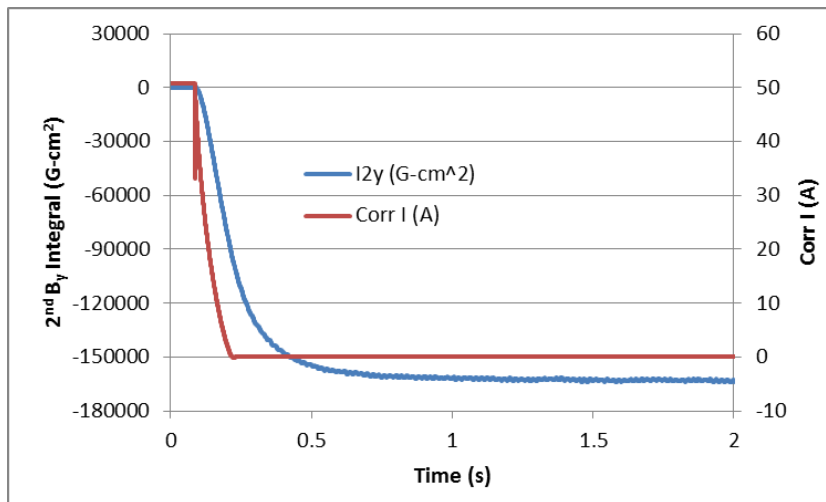
Details of quench properties presented in [12,13]

1st and 2nd Integral response to corrector PS shutdown (worst case for e-beam perturbation)



Loss of corrector power supply with the main continuing to operating would be worse case for beam bump

Change of exit angle $\sim 7 \mu\text{Rad}$ in 0.25 s
Change of exit offset $\sim 70 \mu\text{m}$
Change of average photon trajectory angle $\sim 200 \mu\text{Rad}$



Some observations

- The main coils were energized to the design current of 500 A the first time without a quench.
- The maximum sustained current without quenching was 700 A (at 3.8 K) for two hours with the last hour having 10 W of heat applied to Al beam chamber
- The maximum achieved current was 708 A, this was after a total of about 33 intentional quenches over one month of testing,
- During the course of several weeks of testing, there were no inadvertent quenches while the magnet was energized to between 500 and 600 A.
- Post quench the magnet cores will cool back down in less than 10 minutes, but it takes approximately 30 min for the LHe tank pressure to recover. The tank pressure increases by about 60 Torr during a quench (2 kJ stored energy). Typically we operated the tank pressure near atmosphere at 760 Torr and wanted to keep the pressure below 850 Torr. The maximum LHe tank pressure will have an impact on when the magnet can be re-energized after a quench.
- The magnet didn't quench after applying approximately 45 W of heat to the Al beam chamber over several hours.



Conclusion

- The SCU horizontal magnetic measurement system performed very well for both the Hall probe and coil measurements. Overall design worked very well. We have plans to do some small modifications to ease guide tube alignment.
- The SCU0 magnet performs better for all design parameters except the integrated skew quadrupole component. The design specification is 50 G and the measured value was 120 G at 500 A. Methods to correct for this in longer devices are being explored.
- Phase errors are typically 1 degree rms or less from 100 to 600 A.
- The normal 1st field integrals typically change less than 30 G-cm from 100 to 600 A for both fixed currents and dynamic changes in current.
- The skew 1st field integral changes by less than 40 G-cm from 100 to 600 A
- The normal and skew 2nd field integrals change by less than 8000 G-cm² from 100 to 600 A dependent on the corrector current lookup table.
- Worst case for an e-beam bump would be if the corrector power supply failed and the main supply continued to operate. In this case the average trajectory angle would change by 200 μ Rad, the exit angle by 7 μ Rad, and the exit offset by 70 μ m.
- The cryogenic and magnetic performance of the SCU0 has been remarkable so far.

References

1. C. L. Doose, "Superconducting Undulator Horizontal Magnetic Measurement System Design," Technical Report, [APS 1425029](#), (2011)
2. Y. Ivanyushenkov, M. Abliz, C.L. Doose, M. Kasa, E.M. Trakhtenberg, I.B. Vasserman, N.A. Mezentsev, V.M. Tsukanov, V.K. Lev, "[Development Status of a Magnetic Measurement System for the APS Superconducting Undulator](#)," PAC 2011, Brookhaven National Laboratory (2011), 1286 - 1288.
3. I. Vasserman, Private Communication (2010)
4. I. Vasserman and J. Xu. "A new magnetic field integral measurement system," Technical Report , ANL/APS/TB-49, APS, (2004).
5. T. Tanabe and H. Kitamura. Journal of Synchrotron Radiation, 5, 475–477, (1998).
6. S.H. Kim, R.J. Dejus, C. Doose, R.L. Kustom, E.R. Moog, M. Petra, K.M. Thompson, "Development of a short-period superconducting undulator at APS," Proceedings of the 2003 Particle Accelerator Conference, J. Chew, P. Lucas, and S.Webber, eds., IEEE (2003), 1020 - 1022.
7. S.H. Kim, C.L. Doose, R.L. Kustom, E.R. Moog, "[Development of Short-Period Nb₃Sn Superconducting Undulators for the APS](#)," IEEE T. Appl. Supercon. **18** (2), 431-434 (2008). DOI: 10.1109/TASC.2008.920528
8. Y. Ivanyushenkov, K. Boerste, T. Buffington, C. Doose, Q. Hasse, M. Jaski, M. Kasa, S.H. Kim, R.L. Kustom, E.R. Moog, D. Peters, E.M. Trakhtenberg, I.B. Vasserman, "[Status of R&D on a Superconducting Undulator for the APS](#)," PAC09, IEEE (2010), 313 - 315.
9. C.L. Doose, M. Kasa, S.H. Kim, "[End-Field Analysis and Implementation of Correction Coils for a Short-Period NbTi Superconducting Undulator](#)," PAC 2011, Brookhaven National Laboratory (2011), 1280 - 1282.
10. C. L. Doose, M. Kasa, "Recent Magnetic Measurement Results of the 42 pole prototype SCU Jan 2011," Technical Report, [APSU 1421333](#), (2011)
11. M. Abliz, I. Vasserman, Y. Ivanyushenkov, C. Doose, "[Temperature-Dependent Calibration of Hall Probes at Cryogenic Temperature](#)," PAC 2011, Brookhaven National Laboratory (2011), 1223 - 1225.
12. C.L. Doose, M. Kasa, S.H. Kim, "[Quench Properties of Two Prototype Superconducting Undulators for the Advanced Photon Source](#)," PAC 2011, Brookhaven National Laboratory (2011), 1121 - 1123.
13. S.H. Kim, "Resistive Wall Heating due to Image Current on the Beam Chamber for a Superconducting Undulator," Technical Report ANL/APS/LS-329, (February -2012).

